



HAL
open science

A stochastic model for cell adhesion to the vascular wall

Christèle Etchegaray, Nicolas Meunier

► **To cite this version:**

Christèle Etchegaray, Nicolas Meunier. A stochastic model for cell adhesion to the vascular wall. 2017.
hal-01442975v1

HAL Id: hal-01442975

<https://hal.science/hal-01442975v1>

Preprint submitted on 23 Jan 2017 (v1), last revised 12 Dec 2019 (v3)

HAL is a multi-disciplinary open access archive for the deposit and dissemination of scientific research documents, whether they are published or not. The documents may come from teaching and research institutions in France or abroad, or from public or private research centers.

L'archive ouverte pluridisciplinaire **HAL**, est destinée au dépôt et à la diffusion de documents scientifiques de niveau recherche, publiés ou non, émanant des établissements d'enseignement et de recherche français ou étrangers, des laboratoires publics ou privés.

A stochastic model for cell adhesion to the vascular wall

Christèle Etchegaray* Nicolas Meunier†

Abstract

We present here a minimal mathematical model of the interaction between a cell and the blood vessel wall in shear flow. The bond dynamics in cell adhesion is modeled as a non-linear discrete stochastic process. Performing a renormalization in the spirit of [22, 11], we obtain a continuous model which predicts the existence of a threshold shear velocity associated with cell rolling and a process of firm adhesion that follows the initial rolling.

1 Introduction

Leukocytes adhesion to the vascular wall is a major process involved during inflammation or metastasis invasion [15]. The adhesive interaction between leukocytes and endothelial cells occurs in the presence of the hemodynamic forces exerted on the leukocytes by the blood flow. The first step of interaction happens when enough bonds between the cell and the wall are stabilized so that the cell is slowed down, this is the so called capture phase. Then, leukocytes roll along the stimulated endothelial cells, as new bonds form in the direction of motion and bonds at the back disassemble. This step is mediated by adhesion molecules of the selectin family. During rolling, the leukocytes may also be stimulated, and consequently another family of cell adhesion molecules, the integrins, is activated on the leukocyte surface. The integrins mediate the firm adhesion which slows the cell enough so that it penetrates the vascular wall allowing for the further development of the phenomenon at play (immune response, invasion of tissues by metastatic cells e.g, see for example [27]). It is observed that rolling does not always turn to firm adhesion, and leukocytes may return in the blood flow.

Leukocyte rolling has been studied in vivo and in vitro in flow chambers, in which isolated leukocytes are rolling on either monolayers of cultured

*LMO, Univ. Paris-Sud, CNRS, Université Paris-Saclay, 91405 Orsay, France. & MAP5, CNRS UMR 8145, Université Paris Descartes, 45 rue des Saints Pères 75006 Paris, France. (christele.etchegaray@math.u-psud.fr)

†MAP5, CNRS UMR 8145, Université Paris Descartes, 45 rue des Saints Pères 75006 Paris, France. (nicolas.meunier@parisdescartes.fr)

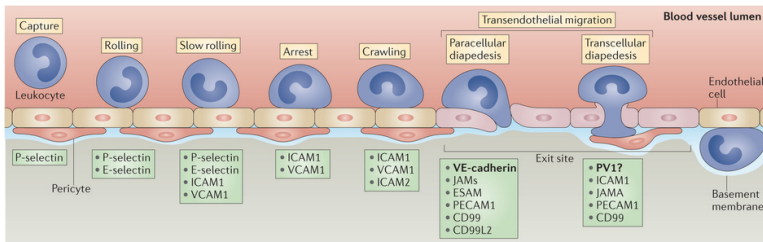


Figure 1: Scheme of the multistep cascade of leukocyte extravasation.

endothelial cells or surfaces coated with selectin or other molecules. It has been observed that the velocities of rolling cells are orders of magnitudes lower than the velocities of non-adherent cells freely moving close to the substratum surface. This indicates adhesive interaction between the rolling cells and the substratum [41].

The rolling motion has been observed to be stochastic both in vivo, [38], and in vitro, [14]. Variation of the rolling velocities of individual cells in time has also been observed for experiments in which the leukocytes roll on a flat surface bearing a uniform layer of ligands, [41]. This suggests that the fluctuation in leukocyte dynamics in the vicinity of the wall is a reflection of the stochastic nature of the adhesive interaction.

The aim of the present paper is to build and study a continuous model to describe the motion of a cell that develops adhesive interaction with the vascular wall. In particular, the model ought to be able to recover the different behaviours observed: the cell stopping or its release in the blood flow. To do so, we start with a minimal discrete stochastic model to describe the individual bond dynamics and then we derive the continuous model by performing a scaling limit. More precisely, in the discrete model that describes the individual bond dynamics, we assume the cell to be a point particle submitted to blood flow with 1D constant velocity. Units of resistive force appear/disappear stochastically and discontinuously in time, following a stochastic jump process. The stochastic character of the dynamics is due to the large number of molecules interacting to form bonds, while the discontinuous dynamics results from the choice of scale. We neglect the growth of an adhesion so that the binding dynamics is discontinuous in time.

Since the number of bonds involved in cellular adhesion is very high, in a second step we let the number of bonds go to infinity while the contribution of each bond to the adhesion force goes to zero. In the spirit of [22, 11] by the renormalization of the population of bonds and its dynamics, we rigorously derive a continuous limiting model for the cellular adhesion dynamics. Depending on the renormalization assumptions, we obtain either a deterministic or a stochastic equation, that we both study. The deterministic model successfully predicts the threshold wall shear stress above which

rolling does not occur and, for some parameter values, it predicts the cell stationary adhesion. We also study the continuous stochastic model and derive information on the time needed for the cell to stop. To do so, in a first step we use a Laplace transform approach for the Cox-Ingersoll-Ross (CIR) process, corresponding to a simplified adhesion dynamics. Then, we derive the cell mean stopping time for the whole dynamics, using a Fokker-Planck equation. We believe that this work is a first step in the construction of a permeability law for leukocytes, characterizing the different regimes that can arise: cells either slip or grip to the wall.

The plan of this article is the following. In Section 3, we detail the construction of the discrete stochastic model for the individual bond dynamics. We provide a mathematical analysis of the discrete model in Section 3. In Section 4, using a renormalization technique we build continuous versions of the model and we exhibit different behaviours according to the chosen renormalization: deterministic or stochastic. In section 4 we give the behaviour of the solution to the deterministic model. Finally, in Section 5, we use the continuous stochastic model to compute the mean time needed for the cell to stop.

2 Previous models - their purpose and structure

There exist several models and approaches for leukocytes adhesion. Each approach has its own particular focus, both in how the adhesion processes are represented and in the purpose and results of the modelling.

The simplest approach to leukocyte adhesion modelling is to ignore cell spatial structure and to assume a step-wise, stop-and-go motion of the leukocyte. In [44] the trajectory of the center of the cell is approximated by a series of rapid steps in between which the cell velocity is zero. Two random variables are used to describe the average distance and lifetime of bond clusters resisting the applied fluid force. Performing some mean field approximation makes it possible to heuristically obtain a Fokker-Planck equation which governs the cell velocity evolution. The drift and diffusion coefficients in the Fokker-Planck equation are heuristically derived from the non smoothed stepping process of cell displacement and expressed in terms of the step size and waiting time of this stepping process. The power of this approach was to be able to predict that the distribution of experimentally derived rolling velocities is influenced by analysis of the variance or dispersion of rolling velocity data acquired under different experimental conditions.

In the same spirit, in the absence of fluid flow, macroscopic models have been developed for cell adhesion force [36]. Bonds are not described individually but as a distribution function. This bonds distribution follows a maturation-rupture equation (also called renewal equation). In the limit of large ligands binding turnover, friction coefficient can be computed [32, 33].

In [17, 18], a simulation model was considered to describe the interplay between hydrodynamic transport and specific adhesion. In these works, the leukocyte is modeled as a hard sphere covered with receptors moving above a planar ligand-bearing wall. The ligand-receptor binding follows a chemical kinetic dynamics according to Bell's law, [5]. Bonds then exert elastic forces on the sphere while the linear shear flow exerts both hydrodynamic force and torque. In [24], the Brownian motion of the sphere is taken into account in order to model the spatial receptor-ligand encountering in more details. Algorithms are given that allow to numerically simulate the cell motion as well as the formation and rupture of bonds between receptors and ligands. The strength of these models is to numerically study the influence of bonds which have formed between receptors and ligands, but easily rupture in response to force, on the motion of the sphere.

The model presented here has some similarities with the model heuristically derived in [44] but takes a more detailed view of the events between the cell and the endothelium in the spirit of [17]. We model the loop between the cell velocity and the bond formation dynamics. This leads to a non-linear stochastic jump process to describe the velocity of the cell center. For this non-linear jump process we proceed to a rigorous derivation of the continuous equation satisfied by the cell velocity. This continuous model allows to analytically study the influence of bonds which have formed between receptors and ligands on the cell motion. In particular, the model predicts that the cell can either develop no bonds with the vascular wall when the shear velocity is high and/or the wall is in a lowly inflamed state with low levels of ligands, or the cell decelerates and rolls on the wall with eventually sufficient high deceleration so that the zero value is reached. We show that there is a well-defined region of parameter space where this dichotomy exists and we provide some quantitative information about the cell dynamics.

3 Construction of the discrete stochastic model

Let us consider a cell (a leukocyte e.g.) carried by the blood flow. We suppose that the size of the gap between the cell and the blood vessel wall is small enough so that bonds between the cell and the vascular wall may continuously form in the contact area. Since the cell is in the vicinity of the wall, we assume that the blood shear flow is 1D, parallel to the vascular wall and with a constant velocity, denoted by $u \in \mathbb{R}_+$.

In previous studies, see [9, 21] e.g., it was shown that approximating the contact area by a simple geometrical figure (a circle or a rectangle) and neglecting the increase of the contact area with the flow shear rate due to cell deformability do not change qualitatively the analysis. Moreover, as suggested in [7], the cell adhesion is primarily determined by physicochemical properties of adhesion proteins and, thus, to a first approximation, we

assume the cell to be a point particle whose position at time $t \geq 0$ is denoted by $x(t)$.

3.1 Velocity model

To describe the cell motion in our model, we use a non-inertial approximation. Indeed, in the limit of low Reynolds number, viscous forces dominate over inertial forces and the momentum equation reduces to the force balance principle:

$$V_t = u - F_t, \quad (1)$$

where $V_t \in \mathbb{R}$ is the cell velocity, u is the blood shear flow and the cell is subjected to a macroscopic resistive force, denoted by $F_t \in \mathbb{R}_+$, induced by the bonds that contribute to decelerating the cell, see Figure 1. The previous equation is valid only for $F_t \leq u$, as for a maximal force the cell stops, and the model is no longer valid.

Depending on the ratio between the adhesion force exerted by the stabilized bonds and the load and torque created by the blood flow, which is characterized by the shear rate, two situations might occur:

- either the adhesion force is strong enough to first capture and then slow down the leukocyte (in that case it allows the cell to roll on the wall),
- or the tension exerted by the blood flow on the bonds is too high and the bonds rupture immediately without capturing the cell.

Modeling leukocyte dynamics near a vessel wall now amounts to modeling the time evolution of the adhesive force F_t .

3.2 Discrete stochastic model for the adhesive force

The resistive force arises from the strength of the cell adhesion to the vessel wall. Cellular adhesion is a macroscopic readout of the forces exerted by the wall on the cell through each bond. Moreover, the formation of each bond is based on a highly complex and dynamic set of microscopic (physical and chemical) reactions [7].

Let us now present the very simple mesoscopic discrete model we will use to describe the individual bond dynamics. We denote by N_t the number of stabilized bonds at time t . We assume that each stabilized bond mediates a unit force in the opposite direction of the moving fluid and we denote by $\gamma > 0$ a global non-dimensionalized friction coefficient. Thus, the total force exerted by all the stabilized bonds writes

$$F_t = \gamma N_t.$$

The quantity N_t is a random variable that we assume to follow a classical birth and death dynamics with creation rate c , dissociation rate d and reproduction rate r as follows.

- We assume that the leukocyte is close enough to the arterial wall to interact so that initialization of adhesion forces occurs. Moreover, interaction arises for a low enough flow velocity, and bonds may appear spontaneously at rate c . The simplest choice consists in using a step function of the blood flow velocity u , with a velocity threshold u^* above which no bond is created: $c(u) = c$ if $u \leq u_*$ and $c(u) = 0$ otherwise. In the following, we will always work with a fixed u , but both configurations will be considered.

Remark 1. *The rate for a single bond formation between two proteins is actually mostly determined by the time the two proteins spend near one another. Therefore, the rate c should depend on the cell velocity when the relative velocity between the cell surface and the wall is non zero. A more realistic choice for c would be to consider a decreasing function of the instantaneous cell velocity V_t . A prototypical behaviour would be given by $c(v) = (u_* - v)_+$ where $(\cdot)_+$ denotes the positive part. Recalling that V_t is related to N_t this would amount to choose a rate c depending on N_t the number of stabilized bonds: $c(n) = (u_* - u + \gamma n)_+$. For such a choice, and assuming that $v \leq u_*$, the dependence on n corresponds to the individual reproduction of the bonds in the birth and death process, that we will consider below.*

- Bonds are mostly organized in complexes of cellular adhesions, resulting in cooperation between proteins located on the cell for the reinforcement of the connection to the wall. Indeed, if there is only a single pair of interacting proteins, when the bond between them breaks, then chances that they will form the bond again are negligible. Now for an adhesion formed by a large number of bonds, when one of them breaks, the unbound proteins do not move apart (as long as this is not the last bond). Therefore, the ruptured bond can be rapidly restored. This reinforcement dynamics can also be inputted to cytoskeletal forces or external stresses [34]. Hence, the natural assumption for the model is to impose a reproduction dynamics for each bond and we denote by r the individual reproduction rate.
- Each bond dissociates at rate d . The average lifetime of an adhesion site changes with the applied tension from the blood flow. Moreover, for a given number of bonds, the faster the cell goes, the more force is exerted on each bond and likely existing bonds are to disassemble. This way, a satisfying choice is to take d as an increasing function of V_t . We choose this relation to be exponential: $d(V_t) = de^{\alpha V_t} = de^{\alpha(u - \gamma N_t)}$,

where d is the unstressed bonds dissociation rate. As the cell velocity is bounded by u , so is the dissociation rate.

Finally to describe the bonds dynamics we will use a birth and death process with the following choice for the rates:

$$c(N_t) = c\mathbb{1}_{u \leq u_*} \text{ with } c > 0, \quad r(N_t) = r > 0, \quad \text{and} \quad d(N_t) = de^{\alpha(u-\gamma N_t)}. \quad (2)$$

The key point here is that the bond dynamics depends on the instantaneous cell velocity. More elaborate dependence could be analyzed (see e.g [32, 33]), in particular involving age dependences to model the bond elasticity (see [16]), but we choose to keep a minimal set of parameters, as for simplicity as for the sake of clarity.

4 Mathematical properties and numerical simulations

In this section we consider general rates and we derive mathematical properties of the discrete stochastic process. We first study the well-posedness character and the infinitesimal generator. Then, we introduce a trajectorial representation for this process. This allows to deduce some moment and martingale properties. Finally we present numerical simulations of the discrete model.

4.1 A population approach

Let $(\Omega, \mathcal{F}, \mathbb{P})$ be a probability space. Denote $\mathbb{D}(\mathbb{R}_+, \mathbb{R}_+)$ the Skorohod space of càdàg functions from \mathbb{R}_+ to \mathbb{R}_+ . We consider the following hypothesis:

Hypothesis 1. *There exist positive constants $\bar{C}, \bar{R}, \bar{D}$ such that*

$$\forall n \in \mathbb{N}_+, \quad 0 \leq c(n) \leq \bar{C}, \quad 0 \leq r(n) \leq \bar{R} \quad \text{and} \quad 0 \leq d(n) \leq \bar{D}.$$

We are interested in the following dynamics:

$$n \mapsto \begin{cases} n + 1 & \text{at rate } \lambda(n) = c(n) + r(n)n, \\ n - 1 & \text{at rate } \mu(n) = d(n)n, \end{cases}$$

together with hypothesis 1, and λ and μ are defined on \mathbb{N} . As a consequence, we can write

$$0 \leq \lambda(n) \leq \bar{C} + \bar{R}n, \quad \text{and} \quad 0 \leq \mu(n) \leq \bar{D}n.$$

Proposition 2 (Well-posedness, infinitesimal generator). *The Markovian jump process $(N_t)_{t \geq 0}$ defined by the transitions above is well defined on \mathbb{R}_+ , and its infinitesimal generator $(Q_{i,j})_{(i,j) \in \mathbb{N}^2}$ writes*

$$Q_{i,i+1} = \lambda(i), \quad Q_{i,i-1} = \mu(i), \quad Q_{i,i} = -(\lambda(i) + \mu(i)), \quad Q_{i,j} = 0 \text{ otherwise.} \quad (3)$$

Proof. This is a classical result that can be found e.g in [11]. \square

4.2 Trajectorial representation

We introduce here a stochastic differential equation for $(N_t)_t$ driven by a Poisson Point Measure. We will show existence and uniqueness of the solution, and prove that it follows the dynamics described before.

Let N_0 be an integer-valued random variable, and $M(ds, dw)$ an independent Poisson Point Measure on \mathbb{R}_+^2 , of intensity measure $ds dw$. Finally, $(\mathcal{F}_t)_{t \geq 0}$ denotes the canonical filtration generated by these objects. Let us construct the $(\mathcal{F}_t)_{t \geq 0}$ -adapted càdlàg process $(N_t)_{t \geq 0}$ as the solution of the following SDE: $\forall t \geq 0$,

$$N_t = N_0 + \int_0^t \int_{\mathbb{R}_+} \left(\mathbf{1}_{0 \leq w \leq \lambda(N_{s-})} - \mathbf{1}_{\lambda(N_{s-}) < w \leq \lambda(N_{s-}) + \mu(N_{s-})} \right) M(ds, dw). \quad (4)$$

This representation is classical (see e.g [13, 8]). The Poisson jumps related to the measure are accepted or rejected thanks to the indicator functions. The variable w is then used as an acceptance parameter in order to get the desired rates for each event.

Proposition 3 (Existence, uniqueness, moments propagation). *Assume hypothesis 1, and that there exists $p \geq 1$ such that $\mathbb{E}[N_0^p] < +\infty$. Then,*

1. $\forall T > 0$,

$$\mathbb{E} \left[\sup_{t \in [0, T]} N_t^p \right] < +\infty,$$

2. *the process $(N_t)_t$ exists and is unique in law.*

Proof. See annex 8. □

Now, the process $(N_t)_t$ is classically a Markov process in the Skorohod space $\mathbb{D}(\mathbb{R}_+, \mathbb{R}_+)$ of càdlàg \mathbb{R}_+ -valued processes, and its infinitesimal generator is defined for all $\Phi : \mathbb{R}_+ \rightarrow \mathbb{R}$ measurable bounded by

$$L\Phi(n) = \lambda(n) [\Phi(n+1) - \Phi(n)] + \mu(n) [\Phi(n-1) - \Phi(n)]. \quad (5)$$

In particular, it corresponds to the dynamics described by (3).

4.3 Martingale property

Markov processes are usually associated with a semimartingale structure. We prove now that for some measurable $\Phi : \mathbb{R}_+ \rightarrow \mathbb{R}$, there exists a martingale $(M_t)_t$ and a finite variation process $(A_t)_t$ such that for all $t \geq 0$, $\Phi(N_t) = \Phi(N_0) + A_t + M_t$.

Theorem 4. *Assume that there exists $p \geq 2$ such that $\mathbb{E}[(N_0)^p] < +\infty$. Then,*

1. for all $\Phi : \mathbb{R}_+ \rightarrow \mathbb{R}$ measurable, for which there exists C such that for all $N \in \mathbb{R}_+$, $|\Phi(N)| + |L\Phi(N)| \leq C(1 + N^p)$,

$$\Phi(N_t) - \Phi(N_0) - \int_0^t L\Phi(N_s) ds \quad (6)$$

is a càdlàg square-integrable $(\mathcal{F}_t)_{t \geq 0}$ -martingale starting from 0.

2. This applies in particular to functions $\Phi : N \mapsto N^q$, for $0 \leq q \leq p$.

As a consequence, the \mathbb{R} -valued process $(M_t)_{t \geq 0}$ defined by

$$M_t = N_t - N_0 - \int_0^t (\lambda(N_s) - \mu(N_s)) ds \quad (7)$$

is a càdlàg square-integrable martingale starting from 0 and of quadratic variation

$$\langle M \rangle_t = \int_0^t (\lambda(N_s) + \mu(N_s)) ds. \quad (8)$$

Proof. See annex 9. □

4.4 Moment equation

Let us now investigate the mean path of this process. Using the martingale formulation, we can write

$$\mathbb{E}[N_t] = \mathbb{E}[N_0] + \int_0^t \mathbb{E}[c(N_s) + (r(N_s) - d(N_s))N_s] ds.$$

It is clear that with the choice of $d(N_t) = de^{\alpha(u-\gamma N_t)}$ (with $N_t \leq u/\gamma$ to ensure the model validity), the resulting nonlinearity would prevent the closure of the previous equation. In the particular case where $c(N_s) = c$, $r(N_s) = r$ and $d(N_s) = d$, we get $\mathbb{E}[N_t] = \mathbb{E}[N_0] + ct + (r-d) \int_0^t \mathbb{E}[N_s] ds$, leading to

$$\mathbb{E}[N_t] = \begin{cases} \mathbb{E}[N_0] + ct & \text{if } r = d, \\ \mathbb{E}[N_0]e^{(r-d)t} + \frac{c}{r-d} (e^{(r-d)t} - 1) & \text{otherwise.} \end{cases}$$

At steady state, one finds

$$\mathbb{E}[N]_\infty := \begin{cases} \frac{c}{d-r} & \text{for } r < d, \\ +\infty & \text{otherwise.} \end{cases}$$

In the second case, the value n^* for which the velocity reaches zero is attained. For the velocity,

$$\mathbb{E}[V]_\infty := \begin{cases} u - \gamma \frac{c}{d-r} & \text{for } r < d, \\ -\infty & \text{otherwise, that is to say the velocity reaches 0.} \end{cases}$$

These results show that it is already possible to get a mean dichotomy behaviour based on the bonds dynamics in the discrete case. In order to get deeper analytical results, we will derive a continuous limiting stochastic process associated to this dynamics.

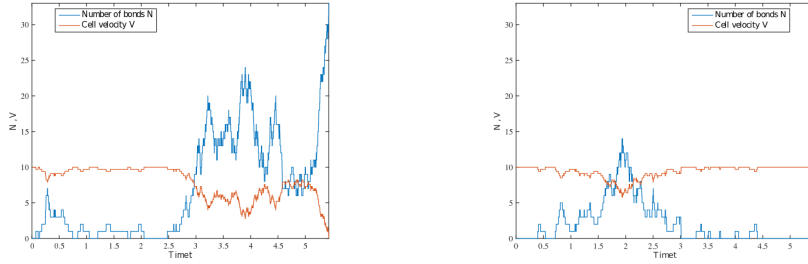


Figure 2: Numerical simulations of the discrete process. Parameters: $u = 10$, $\gamma = 0.3$, $c = 4$, $r = 5$, $d = 3$, $\alpha = 0.1$.

4.5 Numerical Simulations

4.5.1 Algorithm

The bonds population model being a markovian jump process, it is piecewise constant, and the evolution of the process depends only on the present state. Its simulation is therefore straightforward. Consider the population size at time T_k (N_{T_k}). Then,

- the global jump rate is $\varsigma_k = \lambda(N_{T_k}) + \mu(N_{T_k})$. This means that the time before the next event is a random variable following an exponential law of parameter ς_k . A realization of this law gives T_{k+1} .
- Next, we have to determine the type of event occurring: a new bond is created with probability $\frac{\lambda(N_{T_k})}{\varsigma_k}$, while a bond disassemble with probability $\frac{\mu(N_{T_k})}{\varsigma_k}$. Hence, we can compute $N_{T_{k+1}}$.

It is now sufficient to reiterate this procedure to get the time evolution of the process.

4.5.2 Numerical results

Some numerical simulations of the process are displayed in figure 2, for which we chose to stop as soon as the velocity reached zero (or before). It is observed that the velocity either shrinks to zero or remains close to u , depending on the parameter values. Moreover, rolling periods are observed in both cases.

5 Continuous bonds approximations

In this part we separate the scale of the bond dynamics from the one of the cell motion, since the number of bonds is very large, and the binding dynamics very fast compared to the cell displacement. For that purpose, we

let the number of bonds grow to infinity while the individual contribution to the adhesion force shrinks to zero, so that the global adhesive force keeps its range. We also renormalize the dynamics of the bond turnover and this leads to different limiting continuous models.

5.1 Renormalization

Let $K \geq 1$ be a parameter scaling the number of the discrete adhesions we consider. We assume that $\frac{1}{K}$ scales the force generated by each one. This amounts to looking at the adhesion sites at a smaller and smaller scale. Moreover, we assume that the dynamics gets faster and faster. Hence, we consider now K -dependent rates c^K , r^K , and d^K as functions of the corresponding process N_t^K defined by equation (4). We define the renormalized process $(X_t^K)_t \in \mathbb{D}(\mathbb{R}_+, \mathbb{R}_+)$ by

$$X_t^K = \frac{1}{K} N_t^K \in \frac{1}{K} \mathbb{N}. \quad (9)$$

In this subsection, we work with K fixed, and assume that the rates satisfy the following boundedness and continuity hypothesis:

Hypothesis 2. *For all $N \in \mathbb{R}_+$, the following inequalities hold true*

$$0 \leq c^K(N) \leq K\bar{C}, \quad 0 \leq r^K(N) \leq \bar{R} + Ka \quad \text{and} \quad 0 \leq d^K(N) \leq \bar{D} + Ka,$$

where \bar{C} , \bar{R} , \bar{D} and a are positive constants. In addition the rates $N \mapsto c^K(N)$ (resp. $r^K(N)$, resp. $d^K(N)$) are continuous. The global demographic parameters write

$$\lambda^K(N) = c^K(N) + r^K(N)N, \quad \mu^K(N) = d^K(N)N.$$

Markov property By construction, $(X_t^K)_{t \geq 0}$ is also a Markov process, and for $\Phi : \mathbb{R}_+ \rightarrow \mathbb{R}$ measurable bounded, its infinitesimal generator writes

$$L^K \Phi(X) = \lambda^K(KX) \left[\Phi\left(X + \frac{1}{K}\right) - \Phi(X) \right] + \mu^K(KX) \left[\Phi\left(X - \frac{1}{K}\right) - \Phi(X) \right]. \quad (10)$$

As before, for fixed K , we can prove that $(X_t^K)_{t \geq 0}$ satisfies the following proposition.

Proposition 5 (Moment, martingale property). *Assume that there exists $p \geq 2$ such that $\mathbb{E}[(X_0^K)^p] < +\infty$. Then, under hypothesis 2, one has*

1. $\forall T > 0$,

$$\mathbb{E} \left[\sup_{t \in [0, T]} (X_t^K)^p \right] < +\infty, \quad (11)$$

2. for all measurable function $\Phi : \mathbb{R}_+ \rightarrow \mathbb{R}$ for which there exists C such that $\forall X \in \mathbb{R}_+, |\Phi(X)| + |L^K \Phi(X)| \leq C(1 + X^p)$,

$$\Phi(X_t^K) - \Phi(X_0^K) - \int_0^t L^K \Phi(X_s^K) ds \quad (12)$$

is a càdlàg $(\mathcal{F}_t)_{t \geq 0}$ -martingale starting from 0.

3. This applies in particular to functions $\Phi : X \mapsto X^q$, for $0 \leq q \leq p$.

4. The process

$$M_t^K = X_t^K - X_0^K - \int_0^t \frac{1}{K} c^K(KX_s^K) + (r^K(KX_s^K) - d^K(KX_s^K)) X_s^K ds \quad (13)$$

is a càdlàg square-integrable martingale starting from 0 and of quadratic variation

$$\langle M^K \rangle_t = \frac{1}{K} \int_0^t \left\{ \frac{1}{K} c^K(KX_s^K) + (r^K(KX_s^K) + d^K(KX_s^K)) X_s^K \right\} ds. \quad (14)$$

The semimartingale formulation (13) allows us to study the convergence of $(X_t^K)_t$ for $K \rightarrow +\infty$ in $\mathbb{D}(\mathbb{R}_+, \mathbb{R}_+)$ for different renormalizations of the adhesive dynamics.

5.2 Deterministic limits

In this section, we study two sets of parameters leading to deterministic limits. The first one consists in only accelerating the creation rate. In the second one, the whole dynamics is unchanged. For both cases, we consider an additional assumption on the Lipschitz-continuity of the rates.

Hypothesis 3. *The rates are Lipschitz-continuous and satisfy:*

$$0 \leq c^K(KX_t^K) \leq K\bar{C}, \quad r^K(KX_t^K) \leq \bar{R} \quad \text{and} \quad d^K(KX_t^K) \leq \bar{D}.$$

In this context, we can prove the following K -uniform moment property:

Proposition 6. *Assume hypothesis 3 and that there exists $p \geq 1$ such that $\sup_{K>0} \mathbb{E} [(X_0^K)^p] < +\infty$, then*

$$\forall T > 0, \sup_{K>0} \mathbb{E} \left[\sup_{t \in [0, T]} (X_t^K)^p \right] < +\infty. \quad (15)$$

Proof. The proof is similar to the one for proposition 3. Indeed, in equation (13), the coefficient $\frac{1}{K}$ in the creation term compensates for the bound on c^K , and the new bound on r^K is K -independent. As a consequence, taking the supremum of the estimate over $\{K > 0\}$ leads to the result. \square

5.2.1 Accelerated creation

Let us consider the following set of parameters:

$$c^K(KX_t^K) = Kc(X_t^K), \quad r^K(KX_t^K) = r(X_t^K) \quad \text{and} \quad d^K(KX_t^K) = d(X_t^K),$$

where hypothesis 3 is fulfilled. In other words, while we consider an increasing number of smaller adhesions, only their creation is intensified, while their positive effect on the adhesion and their lifetime stay the same.

From the modeling viewpoint such an assumption amounts to consider an increasing number of smaller adhesions, each of them involving a few number of proteins on each side (wall and cell). Note that this corresponds to an intermediate scale (the cell scale) since the clustering process in the adhesion sites is not described. This latter process will be described below, see paragraph 5.3, when the individual dynamics of the bonds is also accelerated.

We prove the following convergence theorem:

Theorem 7. *Assume hypothesis 3. If $X_0^K \xrightarrow{K \rightarrow +\infty} n_0 \in \mathbb{R}_+$ in probability, and if*

$$\sup_{K>0} \mathbb{E} [(X_0^K)^2] < +\infty, \quad (16)$$

then, for $T > 0$, $(X^K)_{K>0}$ converges in law in $\mathbb{D}([0, T], \mathbb{R}_+)$ to the unique continuous function $n \in \mathcal{C}([0, T], \mathbb{R}_+)$ solution to

$$n(t) = n_0 + \int_0^t c(n(s)) + (r(n(s)) - d(n(s)))n(s) ds. \quad (17)$$

Remark 8. *By the Gronwall lemma, one has*

$$\sup_{t \in [0, T]} n(t) \leq (n_0 + \bar{c}T)e^{\bar{c}T} < +\infty,$$

showing that the global density stays finite in finite time.

Proof. The proof is similar to the one in [22, 11]. It is based on a compactness-uniqueness argument. First, the tightness of the sequence of laws $(Q^K)_K$ of $(X^K)_K$ is proved. Then, we establish that for any accumulation point Q , a process X of law Q is almost surely continuous, and solution to equation (17). Finally, the convergence is proved by showing uniqueness in $\mathcal{C}([0, T], \mathbb{R}_+)$ of the solution to (17). Throughout this proof, C will denote a constant that may change during computations, and $C(T)$ a constant depending on T .

Tightness of $(Q^K)_K$ We use the Aldous and Rebolledo criterion [2] as detailed in [22]. Let us denote $(A_t^K)_{t \geq 0}$ the finite variation process related to the semimartingale $(X_t^K)_{t \geq 0}$:

$$A_t^K = X_0^K + \frac{1}{K} \int_0^t c^K(KX_s^K) ds + \int_0^t (r^K(KX_s^K) - d^K(KX_s^K)) X_s^K ds.$$

We need to prove that for all $T > 0$ the following inequalities hold true:

1.

$$\sup_{K>0} \mathbb{E} \left[\sup_{t \in [0, T]} |X_t^K| \right] < +\infty.$$

2. $\forall \varepsilon > 0, \forall \eta > 0, \exists \delta > 0, K_0 \in \mathbb{N}^*$ such that for all sequence $(\sigma_K, \tau_K)_K$ of stopping times with $\sigma_K \leq \tau_K \leq T$,

(a)

$$\sup_{K \geq K_0} \mathbb{P} (|\langle M^K \rangle_{\tau_K} - \langle M^K \rangle_{\sigma_K}| \geq \eta, \tau_K \leq \sigma_K + \delta) \leq \varepsilon,$$

(b)

$$\sup_{K \geq K_0} \mathbb{P} (|A_{\tau_K}^K - A_{\sigma_K}^K| \geq \eta, \tau_K \leq \sigma_K + \delta) \leq \varepsilon.$$

1. The first point is straightforward from proposition 6 together with the assumption (16) made on the initial condition.

2. Take $T > 0, \varepsilon > 0, \eta > 0$ and a sequence of pairs of stopping times $(\sigma_K, \tau_K)_K$ such that $\sigma_K \leq \tau_K \leq T$ and $\tau_K \leq \sigma_K + \delta$.

(a) From equation (14) together with the moment proposition 6, we obtain

$$\mathbb{E} [|\langle M^K \rangle_{\tau_K} - \langle M^K \rangle_{\sigma_K}|] \leq \frac{C}{K} \left(\delta + \mathbb{E} \left[\left| \int_{\sigma_K}^{\tau_K} X_s^K ds \right| \right] \right) \leq \frac{C(T)}{K} \delta.$$

Hence, using the Markov inequality, for all $\varepsilon > 0$, for all $\eta > 0$, there exists δ and K_0 such that 2.a) is satisfied.

(b) Similarly, by proposition 6,

$$\mathbb{E} [|A_{\tau_K}^K - A_{\sigma_K}^K|] \leq C\delta \left(1 + \mathbb{E} [\sup_{[0, T]} X_t^K] \right) \leq C(T)\delta.$$

As before, we conclude by the Markov inequality.

This proves that the sequence $(Q^K)_K$ is uniformly tight in $\mathcal{L}(\mathbb{D}([0, T], \mathbb{R}_+))$.

Identification of the limit : From the Prokhorov theorem we deduce the relative compactness of the family of laws $(Q^K)_K$ on $\mathbb{D}([0, T], \mathbb{R}_+)$. Consider a convergent subsequence, and denote by Q its limit. Next, consider a corresponding sequence of processes $(X^K)_K$ in $\mathbb{D}([0, T], \mathbb{R}_+)$ converging in distribution to $n \in \mathbb{D}([0, T], \mathbb{R}_+)$ of law Q . First, for all $K > 0$, by construction, we know that the jumps of $(X_t^K)_t$ are of the form $1/K$. As a consequence, almost surely, one has

$$\sup_{t \in [0, T]} |X_t^K - X_{t^-}^K| \leq \frac{1}{K},$$

and as $X \mapsto \sup_{t \in [0, T]} |X_t - X_{t-}|$ is continuous from $\mathbb{D}([0, T], \mathbb{R}_+)$ to \mathbb{R}_+ , any process of law Q is almost surely strongly continuous.

Now, let us establish that the process n is solution to equation (17). Using the moment proposition 6, we deduce that $\mathbb{E} \left[\sup_{[0, T]} n_t \right] < +\infty$, which almost surely leads to

$$\sup_{[0, T]} n_t < +\infty. \quad (18)$$

For $T > 0$, take $t \leq T$ and $n \in \mathcal{C}([0, T], \mathbb{R}_+)$. Denote

$$\Psi_t(n) := n_t - n_0 - \int_0^t \{c(n_s) + (r(n_s) - d(n_s))n_s\} ds.$$

We have to prove that for all $t \leq T$, $\mathbb{E}_Q [|\Psi_t(n)|] = 0$. For that purpose, we argue that

1. Since $\mathbb{E} [|\Psi_t(X^K)|] = \mathbb{E} [|\Psi_t(M_t^K)|]$, we have

$$\mathbb{E} [|\Psi_t(X^K)|]^2 \leq \mathbb{E} [|\Psi_t(M_t^K)|^2] = \mathbb{E} [\langle M^K \rangle_t] \leq C \frac{T}{K} \left(1 + \mathbb{E} \left[\sup_{[0, T]} X_t^K \right] \right),$$

and recalling the moment property given in proposition 6, it follows that for all $t \in [0, T]$, $\lim_{K \rightarrow +\infty} \mathbb{E} [|\Psi_t(X^K)|] = 0$.

2. (a) Recalling that n is almost surely continuous and that the parameter rates are continuous, it follows that Ψ_t is continuous in n , and that $\lim_K \Psi_t(X^K) = \Psi_t(n)$ in distribution.
- (b) Moreover, the inequality

$$|\Psi_t(n)| \leq C(T) \left(1 + \sup_{[0, T]} n_s \right)$$

together with proposition 6 yield that $(\Psi_t(X^K))_K$ is uniformly integrable. Hence,

$$\lim_{K \rightarrow +\infty} \mathbb{E} [|\Psi_t(X^K)|] = \mathbb{E} \left[\left| \lim_{K \rightarrow +\infty} \Psi_t(X^K) \right| \right] = \mathbb{E} [|\Psi_t(n)|] = 0.$$

Finally, uniqueness follows from the Lipschitz-continuous hypothesis 3. \square

5.2.2 Non accelerated dynamics

As mentioned before, we can also choose not to accelerate any part of the dynamics. From the modeling viewpoint such an assumption is relevant when the cell velocity is high. In such a case newly formed bonds are instantaneously broken. Note that this situation was already described in the previous section when $u > u_*$. More precisely, consider the following rates:

$$c^K(N_t^K) = c(X_t^K) \quad r^K(N_t^K) = r(X_t^K) \quad d^K(N_t^K) = d(X_t^K)$$

We can prove the following result:

Theorem 9. *Under hypothesis 3, if $X_0^K \xrightarrow{K \rightarrow +\infty} n_0$ in probability on \mathbb{R}_+ for some deterministic n_0 , and*

$$\sup_{K>0} \mathbb{E} [(X_0^K)^2] < +\infty, \quad (19)$$

then $(X^K)_{K>0}$ converges in law in $\mathbb{D}([0, T], \mathbb{R}_+)$ to the unique $n \in \mathcal{C}([0, T], \mathbb{R}_+)$ such that

$$n(t) = n_0 + \int_0^t (r(n(s)) - d(n(s)))n(s)ds, \quad (20)$$

The proof is exactly the same as in theorem 5.2.1.

5.2.3 Analysis of the continuous deterministic equation preserving creation

Let us recall that when creation remains at the limit, the equation writes:

$$n(t) = n_0 + \int_0^t (c(n(s)) + (r(n(s)) - d(n(s)))n(s))ds, \quad (21)$$

where

$$c(n) = c\mathbb{1}_{u < u_*} \text{ with } c > 0, \quad r(n) = r > 0 \quad \text{and} \quad d(n) = de^{\alpha(u-\gamma n)}. \quad (22)$$

The equation satisfied by the cell velocity is

$$v(t) = (u - \gamma n(t))_+. \quad (23)$$

Let us define the function F by: $F(n) = c\mathbb{1}_{u \leq u_*} + (r - de^{\alpha(u-\gamma n)})n$.

Proposition 10. *Let $n_0 \in [0, n^*]$, where n^* corresponds to number of bonds for which the cell velocity vanishes. Assume that the rates are given by (22), then the stationary state n_∞ of (21) satisfies the following:*

1. *If $u > u_*$, then*

(a) *If $u > \frac{1}{\alpha} \ln(\frac{r}{d})$, then there are two stationary states $n_\infty^1 = 0$ and $n_\infty^2 = \frac{u}{\gamma} - \frac{1}{\alpha\gamma} \ln(\frac{r}{d}) > 0$. The smallest is stable and the largest is unstable.*

(b) *Otherwise, then $n_\infty = 0$.*

2. *If $u \leq u_*$, then*

(a) *If $u \leq \frac{1}{\alpha} \ln(\frac{r}{d})$, then $n_\infty = +\infty$.*

- (b) If $u > \frac{1}{\alpha} \ln\left(\frac{r}{d}\right)$, then there exists a unique $0 < \bar{n} < \frac{2}{\alpha\gamma}$ such that $F'(\bar{n}) = 0$ and
- i. If $F(\bar{n}) > 0$, then $n_\infty = +\infty$.
 - ii. If $F(\bar{n}) = 0$, then \bar{n} is the unique stationary solution.
 - iii. If $F(\bar{n}) < 0$, then there exists two stationary solutions n_∞^1 and n_∞^2 , such that $0 < n_\infty^1 < \bar{n} < n_\infty^2 < +\infty$, the smallest being stable and the largest unstable.

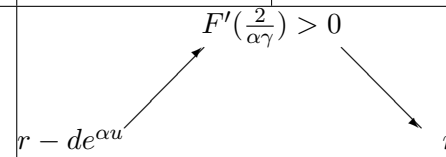
Proof. The case $u > u_*$ follows from a direct computation. Consider the case where $u \leq u_*$, then one has

$$n'(t) = c + \left(r - de^{\alpha(u-\gamma n(t))}\right) n(t) = F(n(t)). \quad (24)$$

A quick computation shows that

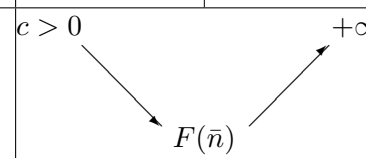
$$\begin{aligned} F'(n) &= r + d(\alpha\gamma n - 1)e^{\alpha(u-\gamma n)}, \\ F''(n) &= \alpha\gamma d(2 - \alpha\gamma n)e^{\alpha(u-\gamma n)}. \end{aligned}$$

We can study the sign of $F'(n)$ and get the following variation table:

n	\emptyset	$\frac{2}{\alpha\gamma}$	$+\infty$
$F''(n)$	+	\emptyset	-
$F'(n)$	$F'(\frac{2}{\alpha\gamma}) > 0$ 		
	$r - de^{\alpha u}$		r

As a consequence,

- If $u \leq \frac{1}{\alpha} \ln\left(\frac{r}{d}\right)$, then $\forall n \in \mathbb{R}_+$, $F(n) \geq c > 0$, hence $n_\infty = +\infty$.
- If $u > \frac{1}{\alpha} \ln\left(\frac{r}{d}\right)$, then there exists a unique $\bar{n} > 0$ such that $F'(\bar{n}) = 0$. Since $\bar{n} < \frac{2}{\alpha\gamma}$, we obtain the following variation table from which the result follows:

n	\emptyset	$\bar{n} < \frac{2}{\alpha\gamma}$	$+\infty$
$F'(n)$	-	\emptyset	+
$F(n)$	$c > 0$ 		
	$c > 0$	$F(\bar{n})$	$+\infty$

Notice that since $u > \frac{1}{\alpha} \ln\left(\frac{r}{d}\right) \Leftrightarrow de^{\alpha u} > r$, both behaviours arise according to the comparison between the reproduction and death rates. \square

Let us comment on these results. First of all, not surprisingly, our model successfully predicts the threshold wall shear stress above which nor capture nor rolling does occur. This is due to the regulation by shear of the number of bonds: the number of bonds falls below one. Moreover, the model predicts existence of cell adhesion bistability, which results from the competition between the two processes taking place in the cell-wall contact area: bond formation and rupture. Finally, the model predicts stationary adhesion which is observed during the leukocytes extravasation.

Remark 11. *Note that if $u_* \geq u > \frac{1}{\alpha} \ln\left(\frac{r}{d}\right)$ the three cases described in the proposition above may occur. Indeed, consider the particular case where $d > r$ and $u = \frac{1-r}{\alpha}$, then $\bar{n} = \frac{u}{\gamma}$ and $F(\bar{n}) = c - \frac{(d-r)^2}{\alpha d \gamma}$ whose sign depends on the value of c . The dynamics is then dependent on the ability of the cell to form bonds at primary contact.*

5.3 Accelerated demography

In this section, we accelerate also the individual dynamics, so that the smaller the scale of adhesion we consider, the faster the dynamics is. From the modeling viewpoint such an assumption amounts to consider an increasing number of smaller adhesions, each of them involving a large number of proteins on each side (wall and cell), so that the attachment/detachment dynamics is faster. Note that this corresponds to the description of the clustering process in the adhesion sites.

For that purpose, let us introduce the parameter $0 < \eta \leq 1$ related to the speed of acceleration compared to the scale reduction. Now, for $K > 0$, and $a > 0$, consider

$$\begin{aligned} c^K(KX_t^K) &= Kc(X_t^K), \\ r^K(KX_t^K) &= r(X_t^K) + K^\eta a, \quad d^K(KX_t^K) = d(X_t^K) + K^\eta a. \end{aligned}$$

The same acceleration for reproduction and death events permits to keep the same bounded individual growth rate $r^K - d^K = r - d$. This way, even if conceptually, each adhesion unity reproduces and dies infinitely faster, its contribution to the global adhesion growth remains the same. The martingale property (13) now writes

$$M_t^K = X_t^K - X_0^K - \int_0^t c(X_s^K) ds - \int_0^t (r(X_s^K) - d(X_s^K)) X_s^K ds \quad (25)$$

is a càdlàg square-integrable martingale starting from 0 and of quadratic variation

$$\langle M^K \rangle_t = \frac{1}{K} \int_0^t \{c(X_s^K) + (r(X_s^K) + d(X_s^K) + 2K^\eta a)X_s^K\} ds. \quad (26)$$

For either $0 < \eta < 1$ or $\eta = 1$, deterministic or stochastic limiting equations will be obtained at the limit. In all cases, we will need moment properties established below. First, we prove a moment estimate uniform in time and K . The method developed in proposition 6 can't be used anymore, as the bound on r is now K -dependent.

Proposition 12. *Consider the process $(X_t^K)_{t \geq 0}$ defined in equation (9). Under hypothesis 2, for $\eta = 1$, and if $\sup_{K > 0} \mathbb{E}[(X_0^K)^2] < +\infty$, then for $T < +\infty$,*

$$\sup_K \sup_{t \in [0, T]} \mathbb{E}[(X_t^K)^2] < +\infty. \quad (27)$$

Proof. Let us use equation (12) for $\Phi(X) = X^2$. We obtain

$$L^K \Phi(X_s^K) = K(c(X_s^K) + X_s^K r(X_s^K))B_+ + K X_s^K d(X_s^K)B_- + K^2 a X_s^K (B_+ + B_-),$$

with $B_+ = (X_s^K + \frac{1}{K})^2 - (X_s^K)^2$ and $B_- = ((X_s^K - \frac{1}{K})^2 - (X_s^K)^2)$. Now, as $B_- \leq 0$, we can neglect the second death terms and study an inequality. Moreover, we compute

$$B_+ = \frac{2}{K} X_s^K + \frac{1}{K^2}, \quad B_- = -\frac{2}{K} X_s^K + \frac{1}{K^2}, \quad B_+ + B_- = \frac{2}{K^2},$$

leading to

$$L^K \Phi(X_s^K) \leq (\bar{C} + \bar{R} X_s^K) \left(2X_s^K + \frac{1}{K} \right) + 2a X_s^K \leq C (1 + X_s^K + (X_s^K)^2).$$

Hence, we can deduce from equation (12) that

$$\begin{aligned} \mathbb{E}[(X_t^K)^2] &= \mathbb{E}[(X_0^K)^2] + \int_0^t \mathbb{E}[L^K \Phi(X_s^K)] ds \\ &\leq \mathbb{E}[(X_0^K)^2] + C \left(t + \int_0^t \mathbb{E}[X_s^K] + \mathbb{E}[(X_s^K)^2] ds \right). \end{aligned}$$

Finally, since $\mathbb{E}[X_s^K] \leq C(1 + \mathbb{E}[(X_t^K)^2])$, by the Gronwall lemma, there exists a constant $C(t)$ such that $\mathbb{E}[(X_t^K)^2] \leq C(t)$, hence

$$\sup_{K > 0} \sup_{t \in [0, T]} \mathbb{E}[(X_t^K)^2] < +\infty.$$

□

We show now a K -uniform control on $\mathbb{E} \left[\sup_{t \in [0, T]} X_t^K \right]$.

Proposition 13. *Consider the process $(X_t^K)_{t \geq 0}$ defined in equation (9) for all $K > 0$. Assume that $\sup_{K > 0} \mathbb{E}[(X_0^K)^2] < +\infty$. Then, for $T < +\infty$,*

$$\sup_K \mathbb{E} \left[\sup_{t \in [0, T]} X_t^K \right] < +\infty. \quad (28)$$

Proof. Recall (13) that rewrites

$$X_t^K = M_t^K + X_0^K + \int_0^t c(X_s^K) + (r(X_s^K) - d(X_s^K)) X_s^K ds.$$

As a consequence,

$$\sup_{t \in [0, T]} X_t^K \leq \sup_{t \in [0, T]} |M_t^K| + X_0^K + \bar{C}T + \bar{R} \int_0^t X_s^K ds.$$

Now, by the Burkholder-Davis-Gundy inequality,

$$\mathbb{E} \left[\sup_{t \in [0, T]} |M_t^K| \right]^2 \leq \mathbb{E} \left[\sup_{t \in [0, T]} |M_t^K|^2 \right] \leq 4\mathbb{E} [|M_T^K|^2] = 4\mathbb{E} [\langle M^K \rangle_T],$$

and as $\mathbb{E}[X_0^K] < +\infty$,

$$\mathbb{E} \left[\sup_{t \in [0, T]} X_t^K \right] \leq 2\mathbb{E} [\langle M^K \rangle_T]^{1/2} + C(T) + \bar{R} \mathbb{E} \left[\int_0^t X_s^K ds \right].$$

We use (14) to get

$$\mathbb{E} [\langle M^K \rangle_T] \leq \bar{C}T + (\bar{R} + \bar{D} + 2a) \int_0^t \mathbb{E} [X_s^K] ds \leq C(T)$$

thanks to (12). We conclude by using the Gronwall lemma. \square

The deterministic case: $0 < \eta < 1$ We consider here the case where the individual dynamics is less accelerated as the scale gets smaller and smaller. As a consequence, the stochastic fluctuations in the adhesion dynamics are not important enough to impact the migration dynamics, and get a deterministic limit. We assume the following:

Hypothesis 4 (Deterministic limit). *For \bar{C} , \bar{R} , \bar{D} positive constants, consider the positive rates*

$$\begin{aligned} c^K(KX_t^K) &= Kc(X_t^K) \leq K\bar{C}, \\ r^K(KX_t^K) &= r(X_t^K) + K\eta a, \quad d^K(KX_t^K) = d(X_t^K) + K\eta a, \end{aligned}$$

with $r(\cdot) \leq \bar{R}$ and $d(\cdot) \leq \bar{D}$. Moreover, c , r and d are Lipschitz-continuous functions.

Theorem 14. *Under hypothesis 4, if for $K \rightarrow +\infty$ the initial measure X_0^K converges in probability on \mathbb{R}_+ to a constant n_0 , and if*

$$\sup_{K > 0} \mathbb{E} [(X_0^K)^2] < +\infty, \quad (29)$$

then $(X^K)_{K>0}$ converges in law in $\mathbb{D}([0, T], \mathbb{R}_+)$ to the unique deterministic function $n \in \mathcal{C}([0, T], \mathbb{R}_+)$ such that

$$n_t = n_0 + \int_0^t \{c(n_s) - (r(n_s) - d(n_s))n_s\} ds. \quad (30)$$

Proof. The proof is similar to the one of theorem 7. Indeed, the only difference is the K^η terms in the reproduction and death terms, but as $\eta < 1$, this doesn't prevent the quadratic variation from going to 0 as K tends to infinity. \square

The stochastic case: $\eta = 1$ Now, we study the case where the binding dynamics is accelerated enough so that stochastic fluctuations remain at the limit. We consider now the following hypothesis:

Hypothesis 5 (Stochastic limit). For $\bar{C}, \bar{R}, \bar{D}$ positive constants,

$$c^K(KX_t^K) = Kc(X_t^K) \leq K\bar{C}, \quad r^K(KX_t^K) = r(X_t^K) + Ka \leq \bar{R} + Ka,$$

$$d^K(KX_t^K) = d(X_t^K) + Ka \leq \bar{D} + Ka$$

Moreover, c, r and d are Lipschitz-continuous.

Theorem 15. Under hypothesis 5, if for $K \rightarrow +\infty$ the initial value X_0^K converges in law to a \mathbb{R}_+ -valued random variable N_0 , with

$$\sup_{K>0} \mathbb{E} [(X_0^K)^2] < +\infty, \quad (31)$$

then $(X^K)_{K>0}$ converges in law in $\mathbb{D}([0, T], \mathbb{R}_+)$ to the continuous process $N = (N_t)_{t \in [0, T]} \in \mathcal{C}([0, T], \mathbb{R}_+)$ solution of

$$dN_t = b(N_t)dt + \sigma(N_t)dB_t \quad (32)$$

with B_t a Brownian Motion, $b(N_t) = c(N_t) + (r(N_t) - d(N_t))N_t$ and $\sigma(N_t) = \sqrt{2aN_t}$.

Proof. The proof is here again based on a compactness-uniqueness argument: we prove that the sequence of laws $(Q^K)_K$ of the processes $(X^K)_K$ is tight. Then, we identify its limiting values as solutions of (32), for which uniqueness is stated.

Uniform tightness of $(Q^K)_K$. As in the proof of theorem 7, denote $(A_t^K)_{t \geq 0}$ the finite variation process related to the semimartingale $(X_t^K)_{t \geq 0}$:

$$A_t^K = X_0^K + \frac{1}{K} \int_0^t c^K(KX_s^K) ds + \int_0^t (r^K(KX_s^K) - d^K(KX_s^K)) X_s^K ds.$$

We need to prove that for all $T > 0$ the following inequalities hold true:

1.

$$\sup_{K>0} \mathbb{E} \left[\sup_{t \in [0, T]} |X_t^K| \right] < +\infty.$$

2. $\forall \varepsilon > 0, \forall \eta > 0, \exists \delta > 0, K_0 \in \mathbb{N}^*$ such that for all sequence $(\sigma_K, \tau_K)_K$ of stopping times with $\sigma_K \leq \tau_K \leq T$,

(a)

$$\sup_{K \geq K_0} \mathbb{P} (|\langle M^K \rangle_{\tau_K} - \langle M^K \rangle_{\sigma_K}| \geq \eta, \tau_K \leq \sigma_K + \delta) \leq \varepsilon,$$

(b)

$$\sup_{K \geq K_0} \mathbb{P} (|A_{\tau_K}^K - A_{\sigma_K}^K| \geq \eta, \tau_K \leq \sigma_K + \delta) \leq \varepsilon.$$

1. The first point is straightforward from proposition 13 together with the assumption (31) made on the initial condition.

2. Take $T > 0, \varepsilon > 0, \eta > 0$ and a sequence of pairs of stopping times $(\sigma_K, \tau_K)_K$ such that $\sigma_K \leq \tau_K \leq T$ and $\tau_K \leq \sigma_K + \delta$.

(a) From equation (14) together with the moment proposition 13, we obtain

$$\begin{aligned} \mathbb{E} [|\langle M^K \rangle_{\tau_K} - \langle M^K \rangle_{\sigma_K}|] &\leq \frac{C}{K} \left(\delta + \mathbb{E} \left[\left| \int_{\sigma_K}^{\tau_K} X_s^K ds \right| \right] \right) \\ &\leq C(T)\delta. \end{aligned}$$

Hence, using the Markov inequality, for all $\varepsilon > 0$, for all $\eta > 0$, there exists δ and K_0 such that 2.a) is satisfied.

(b) Similarly, by proposition 13,

$$\mathbb{E} [|A_{\tau_K}^K - A_{\sigma_K}^K|] \leq C\delta \left(1 + \mathbb{E} [\sup_{[0, T]} X_t^K] \right) \leq C(T)\delta.$$

As before, we conclude by the Markov inequality.

This proves that the sequence $(Q^K)_K$ is uniformly tight in $\mathcal{L}(\mathbb{D}([0, T], \mathbb{R}_+))$.

Identification of the limit. Using the Prokhorov theorem, we can consider a convergent subsequence $(Q^K)_K$, and denote Q its limit. Let $(X^K)_K$ be a corresponding sequence of processes in $\mathbb{D}([0, T], \mathbb{R}_+)$ converging in law to $N \in \mathbb{D}([0, T], \mathbb{R}_+)$. As in the proof of theorem 7, we can show that N is almost surely strongly continuous.

Now, we show that if for $Y = (Y_t)_{t \geq 0} \in \mathbb{D}([0, T], \mathbb{R}_+)$, we write

$$\tilde{M}_t(Y) = Y_t - Y_0 - \int_0^t \{c(Y_s) + (r(Y_s) - d(Y_s))Y_s\} ds, \quad (33)$$

then $\tilde{M}_t(N)$ is a twice-integrable continuous martingale with quadratic variation

$$\langle \tilde{M} \rangle_t = 2a \int_0^t Y_s ds. \quad (34)$$

First, we show that $\tilde{M}(N)$ is a martingale. Take $0 \leq s_1 < \dots < s_n < s < t$, and Φ_1, \dots, Φ_n continuous bounded functions from \mathbb{R} to \mathbb{R} . Define $\Psi : \mathbb{D}([0, T], \mathbb{R}) \rightarrow \mathbb{R}$ by

$$\Psi(Y) = \Phi_1(Y_{s_1}) \dots \Phi_n(Y_{s_n}) [Y_t - Y_s - \int_s^t \{c(Y_s) + (r(Y_s) - d(Y_s)) Y_s\} du].$$

We need to show that

$$\mathbb{E}[\Psi(N)] = 0.$$

This can be made similarly as in the determinist case, and we refer to the proof of theorem 7 for the details.

The new argument in this proof consists in showing that the bracket of \tilde{M} is given by (34).

1. First, consider the K -dependent semimartingale obtained from equation (12) with $\Phi(X^K) = (X^K)^2$, that is related to the generator:

$$\begin{aligned} L^K \Phi(X_s^K) &= 2X_s^K (c(X_s^K) + (r(X_s^K) - d(X_s^K)) X_s^K) \\ &\quad + \frac{1}{K} (c(X_s^K) + (r(X_s^K) + d(X_s^K) + 2Ka) X_s^K). \end{aligned}$$

As in the previous point we can show that we have at the limit the following martingale:

$$\tilde{N}_t = (N_t)^2 - (N_0)^2 - \int_0^t \{2N_s (c(N_s) + (r(N_s) - d(N_s)) N_s) + 2aN_s\} ds.$$

2. Moreover, applying the Itô formula to equation (33) shows that

$$N_t^2 - N_0^2 - \langle \tilde{M} \rangle_t - \int_0^t 2N_s (c(N_s) + (r(N_s) - d(N_s)) N_s) ds$$

is a martingale. We conclude by the uniqueness of the semimartingale decomposition of N_t^2 .

It remains to show the equivalence between the martingale problem (33)-(34) and the SDE (32). This is a consequence of the classical martingale identification

$$M_t = \int_0^t \sqrt{2aN(s)} dB_s,$$

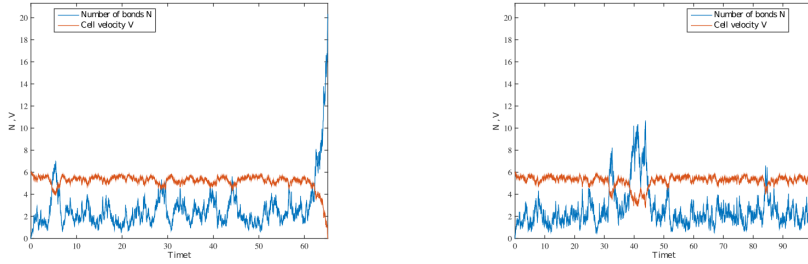


Figure 3: Numerical simulations of the solution of the SDE (32). Parameters: $u = 6$, $\gamma = 0.3$, $c = 4$ (left) and $c = 5$ (right), $r = 5$, $d = 4$, $\alpha = 0.1$, $a = 0.55$.

see for example [23].

Finally, the pathwise uniqueness of the solution to this SDE is classical in 1D since the drift is Lipschitz-continuous and the diffusion coefficient is 1/2-Hölder (see e.g [19]).

□

Remark 16. *The solution is strong and has the strong Markov property.*

Numerical simulations We performed numerical simulations of the SDE (32) with rates as defined in 22, using a symmetrized Euler scheme (taking the absolute value of the classical Euler scheme) in order to preserve the positivity of the process (see e.g [6]). More precisely, the scheme is the following: write $(N_k)_k$ for the discretization of $(N_t)_t$, with N_k corresponding to the time $t_k = k\Delta t$. Then, define

$$N_0 = n_0 \quad (35)$$

$$N_{k+1} = |N_k + b(N_k)\Delta t + \sqrt{2a\Delta t N_k} Z| \quad \text{for } k \geq 0, \quad (36)$$

with $Z \sim \mathcal{N}(0, 1)$. It is proved in [6] that strong L^1 convergence holds for this scheme if

$$\frac{\sigma^2}{8} \left(\frac{2b(0)}{\sigma^2} - 1 \right)^2 > 3P \vee 4\sigma^2,$$

for $P \geq |r - d|$ and $\Delta t \leq \frac{1}{2P}$. This condition allows to deal with the non Lipschitz diffusion coefficient, and rewrites in our case

$$\frac{a}{4} \left(\frac{c}{a} - 1 \right)^2 > 3P \vee 8a.$$

As an example, $\frac{a}{4} \left(\frac{c}{a} - 1 \right)^2 > 8a$ is equivalent to $\left(\frac{c}{a} - 1 \right)^2 > 32$, that is verified for $c > 7a$. The numerical simulations are displayed in figure 3.

6 Stopping time

The rolling motion of individual cells has been observed to fluctuate randomly both in vivo and in vitro, hence it is natural to study in more details the stochastic limit continuous model previously obtained (after a renormalization procedure). In particular we are interested in the probability for a rolling cell to stop, that is to say for the velocity to reach 0. More precisely, in this section we will compute the mean time T_{n^*} needed for the process to reach $n^* := u/\gamma$ starting from n_0 (say 0). Hence, we focus here on the process $(N_t)_{t \leq T_{n^*}}$, for which almost surely, $N_t \leq n^*$. We start by general remarks on the stochastic differential equation (32).

6.1 General remarks

Positivity Even if we obtained a positive solution in the construction of the last section, we can also show positivity in general if $b(n) \geq 0$ for all $n \geq 0$, and for a positive initial state (see the 1D comparison principle in [23] e.g.).

Change of variable The Itô formula allows us to write SDE (32) on N -dependent quantities.

- For $Y_t = \sqrt{N_t} \in (0, +\infty)$, we can show that

$$dY_t = \frac{b(Y_t^2) - a/2}{2Y_t} dt + \sqrt{\frac{a}{2}} dB_t.$$

The diffusion coefficient is now non-degenerate, but the 0-state is excluded.

- For $V_t = u - \gamma N_t \in [0, u]$ if $N_t \in [0, n^*]$, we obtain

$$dV_t = (u(d(N_t) - r(N_t)) - \gamma c(N_t) + (r(N_t) - d(N_t))V_t) dt + \sqrt{2a\gamma(u - V_t)} dB_t. \quad (37)$$

Using this equation is tempting, as we are interested in the time needed for this quantity to reach 0. However, the diffusion coefficient is now less simple than the one for $(N_t)_t$, as we will see in the sequel.

6.2 Constant rates: the CIR process

For constant rates, the model given by (32) reduces to a CIR process, see [12, 40, 19]:

$$dN_t = (c + (r - d)N_t) dt + \sqrt{2aN_t} dB_t, \quad (38)$$

with $c > 0$, $a > 0$ and $r - d \in \mathbb{R}$. It is known for demographical processes that the diffusion limit of discrete branching processes with immigration

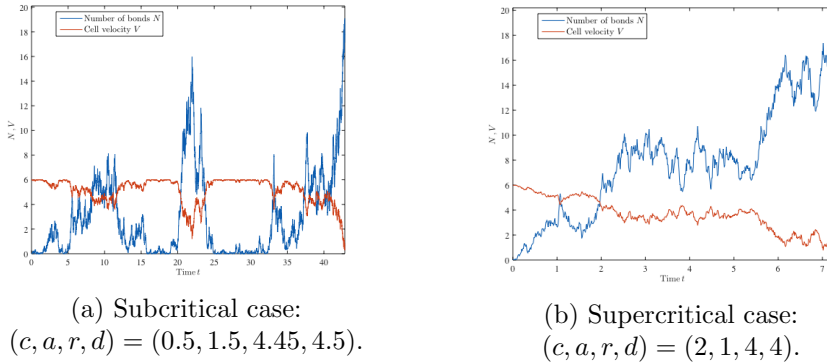


Figure 4: Numerical simulations of the CIR process (38).

results in such processes [3]. Simulations of this process are displayed in figure 4. In this case, the adhesion dynamics is not directly related to the cell velocity, nor on the proximity with the vessel wall. Different behaviours may occur only based on the range of the dynamics: if too low compared to the blood blow, the cell does not stop, and does so for a large enough adhesive dynamics.

6.2.1 Some generalities

In this paragraph, we give some classical results about the CIR process. For more details we refer to [12, 40].

Reaching zero: As mentioned in [12], for $c > 0$ and a positive initial state, $\{N = 0\}$ is naturally a reflective barrier for the process (38). We can also provide information about the probability to hit 0, depending on the quantity $\delta := \frac{2c}{a}$, or equivalently on the comparison between a and c : denote \mathbb{P}^0 the probability to hit 0 in finite time, then one has

$$\begin{array}{c|c|c}
 c < a & & c \geq a \\
 r - d \leq 0 & r - d > 0 & \\
 \hline
 \mathbb{P}^0 = 1 & \mathbb{P}^0 \in (0, 1) & \mathbb{P}^0 = 0
 \end{array}$$

These results can be intuitively understood following the correspondance between CIR processes and Orstein-Uhlenbeck processes for $r - d < 0$. Indeed, consider D such processes (X^1, \dots, X^D) such that $\forall i = 1, \dots, D$,

$$dX_t^i = -\frac{1}{2}\beta X_t^i dt + \frac{1}{2}\sigma dB_t^i,$$

with $(B^i)_i \in \{1, \dots, D\}$ independent Brownian motions and $\beta > 0$. Each process follows a stochastic dynamics that is drifted to zero. Now, similarly

as for Brownian motion, for $D = 1$, the process almost surely hits zero infinitely many times, while for $D \geq 2$, it has a null probability of reaching zero even once.

Using the Itô formula, it is possible to write the SDE that verifies the squared euclidean norm of (X^1, \dots, X^D) , that is to say $R = (X^1)^2 + \dots + (X^D)^2$: we have

$$dR_t = \left(\frac{\sigma^2 D}{4} - \beta R_t \right) dt + \sigma \sqrt{R(t)} dB_t,$$

with B a Brownian motion. Then, denoting $D = 4c/\sigma^2 > 0$, where $\sigma^2 = 2a$, it is possible to derive equation (38) with $r - d = -\beta \leq 0$. Therefore, if D is an integer, the CIR process admits a representation as the squared norm of D Ornstein-Uhlenbeck processes. More generally, the CIR process relates rigorously to the Squared Radial Ornstein-Uhlenbeck process, as it will be precised below.

Remark 17. *It is also possible to relate a CIR process to a Squared Bessel process by a space-time transformation. This process is itself in correspondance with a Squared Radial Ornstein-Uhlenbeck process. Take S a squared Bessel process of dimension $\delta \geq 0$ (denoted $BESQ^\delta$). For a fixed initial condition, it is the unique strong solution of the SDE*

$$dS_t = \delta dt + 2\sqrt{S_t} dB_t. \quad (39)$$

Now, for $\delta = \frac{4c}{2a} = \frac{2c}{a}$, the correspondance between N and S writes

$$N_t = e^{(r-d)t} S_{\frac{a}{2(r-d)}(1-e^{-(r-d)t})}.$$

For $\delta \in \mathbb{N}$, a squared Bessel process also admits a representation as the square norm of a δ -dimensional Brownian motion. Therefore, the previous result can be deduced by the same reasoning [12].

Distribution: It is known that for $\delta = \frac{2c}{a} \in \mathbb{N}$ and $r - d < 0$, we have

$$N_t | n_0 = \frac{(1 - e^{(r-d)t}) 2a}{2(d-r)} Y_t,$$

with Y_t following a non-central chi-square distribution with δ degrees of freedom, and a non-centrality parameter $\xi_t = n_0 \frac{2(d-r)}{(1-e^{(r-d)t})a} e^{(r-d)t}$. This also results from the representation as the squared euclidean norm of a δ -dimensional Ornstein-Uhlenbeck process. The integral form of the SDE (38) allows to compute the mean solution directly, and the variance of the solution (using additionally the Ito formula). We compute

$$\begin{aligned}\mathbb{E}[N_t|n_0] &= n_0 e^{(r-d)t} + \frac{c}{d-r} \left(1 - e^{(r-d)t}\right), \\ \text{Var}(N_t|n_0) &= n_0 \frac{2a}{d-r} \left(e^{(r-d)t} - e^{2(r-d)t}\right) + \frac{ac}{(d-r)^2} \left(1 - e^{(r-d)t}\right)^2.\end{aligned}$$

The corresponding probability density p_{n_0} writes for $n \geq 0$, $n_0 > 0$ and $\kappa_t = \frac{d-r}{(1-e^{(r-d)t})a}$:

$$p_{n_0}(n; k, \xi_t) = \kappa_t \left(\frac{n}{n_0 e^{(r-d)t}}\right)^{\frac{c}{a}-1} e^{-\kappa_t [n_0 e^{(r-d)t} + n]} I_{\frac{c}{a}-1} \left(2\kappa_t \sqrt{n_0 n e^{(r-d)t}}\right),$$

where I_α is the modified Bessel function of the first kind whose definition we recall now:

$$I_\alpha(x) := \sum_{m=0}^{\infty} \frac{1}{m! \Gamma(m + \alpha + 1)} \left(\frac{x}{2}\right)^{2m+\alpha},$$

where Γ is the Gamma function $\Gamma(t) = \int_0^\infty x^{t-1} e^{-x} dx$.

A stationary distribution exists if and only if $r - d < 0$ [19]. In that case, the previous approach gives a possible stationary probability density. Then, writing the Fokker-Planck equation associated to equation (38), we can check that the stationary density writes

$$p_\infty(n) = \left(\frac{d-r}{a}\right)^{\frac{c}{a}} \frac{1}{\Gamma\left(\frac{c}{a}\right)} n^{\frac{c}{a}-1} e^{\frac{r-d}{a}n}.$$

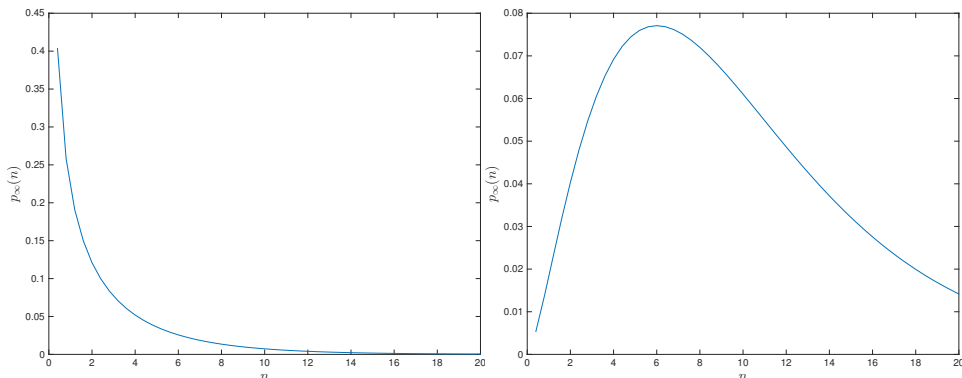
It can be noticed that

$$p_\infty(n) = \mathcal{N} e^{-\varphi(n)}$$

for $\varphi(n) = \left(1 - \frac{c}{a}\right) \ln(n) + \frac{d-r}{a}n$ the corresponding potential, and \mathcal{N} a normalization constant. Simulations are displayed in figure 5.

Time to reach n^* : For the CIR process, it is possible to explicit the Laplace transform of the first hitting time of any value, starting at a given point [12, 26]. It is not possible to proceed to its inversion analytically. Numerical inversion procedures exist, and some of them are compared in [26]. They do not always provide satisfactory results: the integral of the output may not be equal to one, and negative values may appear. The procedure proposed by [1] seems satisfactory in this viewpoint. However in [28], a spectral expansion of the probability density is used, and we will follow this method.

We start by giving an outline of the ideas leading to the expressions of the Laplace transform of first hitting times of CIR processes. For more details we refer to [12].



(a) Subcritical case: $c = 1$, $a = 2$. (b) Supercritical case: $c = 5$, $a = 2$.

Figure 5: Numerical simulations of the stationary probability density of the CIR process for $u = 6$, $\eta = 0.3$, $\alpha = 0.1$, $r = 4$, and $d = 4.5$.

We exploit the rigorous link that exists between the CIR process and the Squared δ -dimensional Radial Ornstein-Uhlenbeck process of parameter $-\kappa$, denoted SROU in the sequel, corresponding to the SDE

$$dZ_t = (\delta - 2\kappa Z_t)dt + 2\sqrt{Z_t} dB_t. \quad (40)$$

Recalling equation (38), we obtain the SROU using the change of variable $Z_t = \frac{2}{a}Nt$. Then, we have $\delta = \frac{2c}{a}$ and $-2\kappa = r - d$.

Now, the squared root of a δ -SROU process is called a δ -dimensional Radial Ornstein-Uhlenbeck process (or δ -ROU, denoted by $(R_t)_t$). A Girsanov theorem relates its law and the law of a Bessel process [12]. Briefly, the Laplace transform of first hitting times for Bessel process are obtained by exploiting time-reversal arguments. These expressions transfer to ROU processes, allowing to get explicit Laplace transforms in the case of CIR processes. Detailed proofs are displayed in [12]. Take $x, y \geq 0$, and denote ${}^P T_{x \rightarrow y}$ the random variable corresponding to the time needed for a process P to reach y starting from x . Then,

$${}^N T_{x \rightarrow y} \stackrel{\text{law}}{=} Z T_{\frac{2x}{a} \rightarrow \frac{2y}{a}} \stackrel{\text{law}}{=} R T_{\sqrt{\frac{2x}{a}} \rightarrow \sqrt{\frac{2y}{a}}}.$$

Let us introduce now the Whittaker's functions

$$M_{k,\mu}(z) := z^{\mu+1/2} e^{-z/2} \Phi(\mu - k + 1/2, 2\mu + 1; z),$$

and the Kummer confluent hypergeometric function defined for $b \notin \mathbb{Z}^-$,

$$\Phi(a, b; z) := \sum_{j=0}^{\infty} \frac{(a)_j}{(b)_j} \frac{z^j}{j!},$$

with $(r)_0 = 1$, $(r)_j = \frac{\Gamma(r+j)}{\Gamma(r)} = r(r+1)\dots(r+j-1)$ for $j \geq 1$. Moreover, $I_\nu(\cdot)$ is the first modified Bessel function of order ν . Then, the following expressions are verified [12].

Theorem 18 (0 to x , [12]). *Denote $T_x = \inf\{t | R_t = x, R_0 = 0\}$ for $(R_t)_t$ a δ -ROU process with parameter $-\kappa$ (we drop the R superscript for simplicity). Then, its Laplace Transform writes*

$$\begin{aligned} \mathbb{E}_0 [e^{-\alpha T_x}] &= \frac{2^{\alpha/\kappa - \nu - 1} x^\nu \Gamma(\alpha/(2\kappa)) \kappa^{\alpha/(2\kappa)}}{\Gamma(\nu + 1) \int_0^{+\infty} I_\nu(\gamma x) e^{-\gamma^2/(4\kappa)} \gamma^{\alpha/\kappa - \nu - 1} d\gamma} \\ &= \frac{(\sqrt{\kappa}x)^{\nu+1} e^{-\kappa x^2/2}}{M_{(-\alpha/\kappa + \nu + 1)/2, \nu/2}(\kappa x^2)} \\ &= \frac{1}{\Phi(\alpha/(2\kappa), \nu + 1; \kappa x^2)}. \end{aligned}$$

Then, since for $0 < y < x$, we have $T_x = T_y + T_{y \rightarrow x}$ in law, and as by the strong Markov property, T_y and $T_{y \rightarrow x}$ are independent, we get the following corollary.

Corollary 1 ($0 < y < x$ to x [12]).

$$\begin{aligned} \mathbb{E}_y [e^{-\alpha T_x}] &= \left(\frac{x}{y}\right)^{\nu+1} e^{\kappa(y^2 - x^2)/2} \frac{M_{(-\alpha/\kappa + \nu + 1)/2, \nu/2}(\kappa y^2)}{M_{(-\alpha/\kappa + \nu + 1)/2, \nu/2}(\kappa x^2)} \\ &= \frac{\Phi(\alpha/(2\kappa), \nu + 1; \kappa y^2)}{\Phi(\alpha/(2\kappa), \nu + 1; \kappa x^2)}. \end{aligned}$$

Remark 19. *Analogous results exist for the case $0 < x < y$, but are not useful for our purpose.*

We follow now the work of [28, 29] to compute numerically the first hitting time density using an eigenfunction decomposition, following an approach used for diffusions [10, 20, 31]. For the CIR process, it is established in [30, 29] that the same type of decomposition holds. More precisely, the infinitesimal generator \mathcal{G} associated to the CIR diffusion (38) writes for $y > 0$

$$(\mathcal{G}u)(y) = \frac{1}{2} \sigma^2 y u''(y) + (c + (r - d)y) u'(y),$$

with $\sigma^2 = 2a$. For $c/a < 1$, the origin is attainable and instantaneously reflecting. In this case, the state space is $I = [0, +\infty)$, and we have the boundary condition at zero

$$\lim_{y \downarrow 0} \frac{u'(y)}{s(y)} = 0, \quad (41)$$

where $s(y) = y^{-c/a} \exp(-(r - d)y/a)$. For $c/a \geq 1$, the origin is unattainable, $I = (0, +\infty)$, and the previous boundary condition is directly satisfied.

The infinitesimal generator is thus defined on $D(\mathcal{G}) := \{u \in \mathcal{C}_b(\mathbb{R}) : \mathcal{G}(u) \in \mathcal{C}_b(\mathbb{R}) \text{ and the condition (41) holds.}\}$. The infinitesimal generator can be rewritten for $x \in [0, +\infty)$,

$$(\mathcal{G}u)(y) = m(y) \left(\frac{u'(y)}{s(y)} \right)',$$

where $m(y) = \frac{1}{ays(y)}$. Notice that s and m are continuous and strictly positive on $(0, +\infty)$.

Since the CIR process admits a stationary distribution (for $r - d < 0$), it is positively recurrent: $\mathbb{P}_y(T_{y \rightarrow x} < +\infty) = 1$ and $\mathbb{E}_y[T_{y \rightarrow x}] < +\infty$. We apply now a result proved in [29] and applied in [28] to the CIR process.

Proposition 20. [29] *For $y < x \in I$ and $t > 0$, we have*

$$\mathbb{P}_y(t < T_{y \rightarrow x}) = \sum_{n=1}^{+\infty} o_n e^{-\lambda_n t}, \quad (42)$$

with $0 < \lambda_1 < \lambda_2 < \dots$, $\lambda_n \rightarrow_{n \rightarrow +\infty} +\infty$. The families $\{\lambda_n\}_n$ and $\{o_n\}_n$ are defined as follows.

Let us introduce the Sturm-Liouville problem associated to \mathcal{G} :

$$-\mathcal{G}u = \lambda u, \quad (43)$$

for $\lambda \in \mathbb{C}$. Denote $\psi(y, \lambda)$ the unique (up to a multiplicative constant) non-trivial solution of (43), square-integrable with $m(y)$ near $\{y = 0\}$, satisfying the boundary condition (41), and such that $(y, \lambda) \mapsto \psi(y, \lambda)$, $\psi_y(y, \lambda)$ are continuous in $(0, x] \times \mathbb{C}$, and continuous on \mathbb{C} as functions of λ for $y < x$ fixed.

Then, equipping equation (43) of the Dirichlet boundary condition $u(y) = 0$, the family $\{\lambda_n\}_{n \in \mathbb{N}^*}$ is defined as the set of simple positive zeros of the solution:

$$\psi(y, \lambda_n) = 0. \quad (44)$$

Now, $\{o_n\}_{n \in \mathbb{N}^*}$ is defined by

$$o_n = \frac{-\psi(x, \lambda_n)}{\lambda_n \psi_\lambda(y, \lambda_n)}. \quad (45)$$

We state now the result of [28] that gives explicit expressions for $\{\lambda_n\}_{n \in \mathbb{N}^*}$ and $\{o_n\}_{n \in \mathbb{N}^*}$, as well as a series expansion for the first hitting time density $f_{T_{y \rightarrow x}}$. Its uniform convergence is a consequence of estimates given on λ_n and o_n .

Proposition 21. [28] *For $0 < x < y \in I$, and $t > 0$ we have*

$$f_{T_{y \rightarrow x}}(t) = \sum_{n=1}^{+\infty} o_n \lambda_n e^{-\lambda_n t}, \quad (46)$$

with uniform convergence on $[t_0, +\infty)$, $t_0 > 0$, and $0 < \lambda_1 < \dots$, with $\lambda_n \xrightarrow{n \rightarrow +\infty} +\infty$. More precisely, recall that $\Phi(w_1; w_2; w_3)$ denotes the Kummer confluent hypergeometric function. Then, for

$$\bar{y} := -\frac{r-d}{a}y, \quad \bar{x} := -\frac{r-d}{a}x, \quad s_n := \frac{\lambda_n}{r-d},$$

with $\{s_n\}$ such that $0 > a_1 > \dots$, and $s_n \xrightarrow{n \rightarrow +\infty} -\infty$, $\{s_n\}_n$ are the negative roots of $\varphi(\cdot; c/a; \bar{x}) = 0$. The family $\{o_n\}_n$ is then defined by

$$o_n = -\frac{\Phi(s_n; c/a; \bar{y})}{s_n \partial_s (\Phi(s_n; c/a; \bar{x}))}. \quad (47)$$

Moreover, the following large- n asymptotics hold:

$$\lambda_n \underset{n \rightarrow +\infty}{\sim} \frac{(d-r)\pi^2}{4\bar{x}} \left(n + \frac{c}{2a} - \frac{3}{4} \right)^2 - \frac{(r-d)c}{2a}, \quad (48)$$

as well as

$$o_n \underset{n \rightarrow +\infty}{\sim} \frac{(-1)^{n+1} 2\pi(n + c/(2a) - 3/4)}{\pi^2(n + c/(2a) - 3/4)^2 - \frac{2c}{a}\bar{x}} \times e^{\frac{1}{2}(\bar{y}-\bar{x})} \left(\frac{\bar{y}}{\bar{x}} \right)^{\frac{1}{4} - \frac{c}{2a}} \cos \left(\pi \left(n + \frac{c}{2a} - \frac{3}{4} \right) \sqrt{\frac{\bar{y}}{\bar{x}} - \frac{\pi c}{2a} + \frac{\pi}{4}} \right). \quad (49)$$

Therefore, the proposed numerical method requires to compute the set of negative roots of φ to get approximations of the families $\{\lambda_n\}_n$ and $\{o_n\}_n$. The choice of the level of truncation for the approximation of (46) can be made using the following estimate resulting from the expressions above:

$$\left| o_n \lambda_N e^{-\lambda_N t_0} \right|_{N \rightarrow +\infty} \sim A N e^{-B N^2 t_0},$$

for

$$A = \frac{2a\pi}{4x} e^{\frac{\bar{y}-\bar{x}}{2}} \left(\frac{x}{y} \right)^{\frac{1}{4} - \frac{c}{2a}}, \quad B = \frac{a\pi^2}{4x}.$$

Linetsky also remarks that using the large- n estimates (48)-(49) instead of computing zeros of the Kummer function provides quite satisfactory results, in particular for c/a small. For a better accuracy, one can also use the exact expression for the first term, then the estimates. The following numerical simulation was performed using only the asymptotic expansion of λ_n and o_n even for n small, since it is observed that this approximation does not change qualitatively the profile (see figure 6). Obviously, in this case, the obtained function is not a probability density. An inconsistency tends to appear near $\{t = 0\}$ due to the approximation, but the overall shape was conserved.

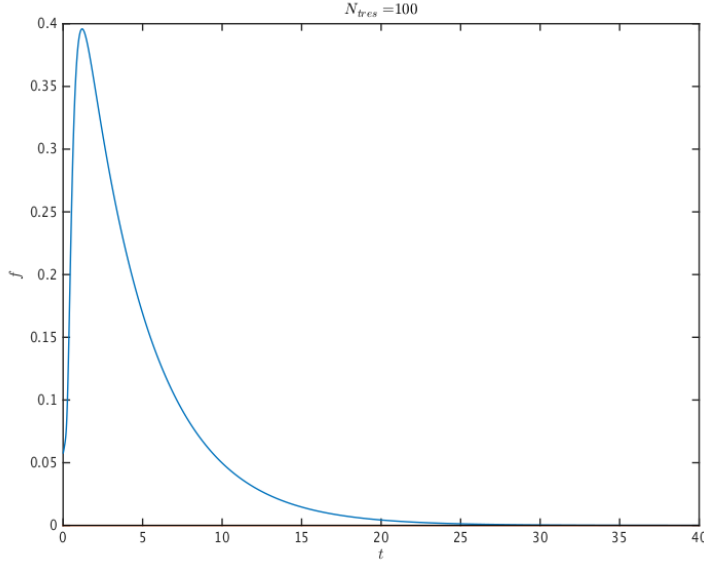


Figure 6: Numerical simulation of an asymptotic spectral decomposition of the probability density of the first hitting time of 1 of a CIR process starting at 0.01. Parameters: $\Delta t = 0.01$, $c = 0.45$, $a = 0.5$, $r = 0.2$ and $d = 1$. The sum is truncated at $N_{tres} = 100$.

6.3 General rates

Let us now focus on the general case of equation (32), assuming hypothesis 5. The first result to state consists in using the 1D comparison result that was already mentioned.

6.3.1 Comparison principle

We assume $0 \leq n_0 < n^*$, hence before the hitting time of n^* we can assume $d(N_t) \leq \underline{D} = d$ (as $u - \gamma n^* = 0$).

Using the bounds on the parameters, it is possible to use a 1D comparison principle (see e.g [37]) to deduce bounds on the hitting time of n^* for our process. We have

$$c + (r - \underbrace{de^{\alpha u}}_{\underline{D}})N_t \leq b(N_t) \leq c + (r - \underbrace{d}_{\underline{D}})N_t,$$

for $N_t \in [0, n^*]$. Denote \bar{N} (resp. \underline{N}) the solution related to the death rate \bar{D} (resp. \underline{D}). Almost surely, for $t \in [0, T_{n^*}]$,

$$\underline{n}_t \leq n_t \leq \bar{n}_t,$$

and for the same initial condition $0 \leq n_0 < n^*$, almost surely,

$$\bar{N}T_{n^*} \leq N T_{n^*} \leq \underline{N}T_{n^*}.$$

However, these bounds are not precise enough for our study, and we develop in the following a Fokker-Planck approach.

6.3.2 The Fokker-planck approach

We associate to the SDE (32) the Fokker-Planck equation on $p(n, t) := p(n, t|n_0, t_0)$ the probability density of $(N_t)_t$ conditionnally to its initial condition:

$$\frac{\partial p(n, t)}{\partial t} = \frac{\partial}{\partial n} \underbrace{\left(-b(n)p(n, t) + \frac{1}{2} \frac{\partial}{\partial n} (\sigma^2(n)p(n, t)) \right)}_{\mathbf{J}(n, t)}, \quad (50)$$

where we recall that $b(n) = c + (r(n) - d(n))n$, while $\sigma(n) = \sqrt{2an}$ and $\mathbf{J}(n, t)$ is the associated probability current. The natural boundary conditions are the following:

$$\begin{aligned} \mathbf{J}(0, t) &= 0, \\ \lim_{n \rightarrow +\infty} p(n, t) &= 0, \\ p(n, 0) &= \delta_{n=n_0}. \end{aligned}$$

We are interested in the time necessary for the process to reach the value $n^* > 0$ if it starts at $n_0 \in (0, n^*)$, and with 0 a reflecting barrier. This question can be adressed by considering the Fokker-Planck equation on $(0, n^*)$ with 0 reflecting and n^* an absorbing barrier. More precisely, write $G(n_0, t)$ the probability that a particle starting at n_0 is still in $(0, n^*)$ at time t . Then,

$$G(n_0, t) = \int_0^{n^*} p(n, t|n_0, 0) dn = \mathbb{P}(T \geq t),$$

where T is the exit time from $(0, n^*)$.

Since the dynamics is homogeneous in time, we deduce that $p(n, t|n_0, 0) = p(n, 0|n_0, -t)$ and $n_0 \mapsto p(n, t|n_0, 0)$ satisfy the backward Fokker-Planck equation:

$$\frac{\partial p(n, t|n_0, 0)}{\partial t} = b(n_0) \frac{\partial}{\partial n_0} p(n, t|n_0, 0) + \frac{1}{2} \sigma^2(n_0) \frac{\partial^2}{\partial n_0^2} p(n, t|n_0, 0), \quad (51)$$

and that $(n_0, t) \mapsto G(n_0, t)$ satisfies

$$\frac{\partial G(n_0, t)}{\partial t} = b(n_0) \frac{\partial}{\partial n_0} G(n_0, t) + \frac{1}{2} \sigma^2(n_0) \frac{\partial^2}{\partial n_0^2} G(n_0, t). \quad (52)$$

The initial and boundary conditions are the following:

$$\begin{aligned} G(n_0, 0) &= \int_0^{n^*} \delta(n - n_0) dn = \mathbf{1}_{[0, n^*]}(n_0), \\ \frac{\partial}{\partial n_0} G(0, t) &= 0, \\ G(n^*, t) &= 0. \end{aligned}$$

Take $f : \mathbb{R} \mapsto \mathbb{R}_+$ non-decreasing and \mathcal{C}^1 . Then, classically, $\mathbb{E}[f(T)] = \int_0^{+\infty} f'(t) \mathbb{P}(T > t) dt = \int_0^{+\infty} f'(t) G(n_0, t) dt$. Hence, we get for $k > 1$,

$$\begin{aligned} \tau(n_0) &:= \mathbb{E}[T] = \int_0^{+\infty} G(n_0, t) dt, \\ \tau_k(n_0) &:= \mathbb{E}[T^k] = k \int_0^{+\infty} t^{k-1} G(n_0, t) dt. \end{aligned}$$

Finally, by integration of equation (52) in time, we get ODEs on the family $(\tau_k)_{k \geq 1}$:

$$\begin{cases} b(n_0) \tau'(n_0) + \frac{1}{2} \sigma^2(n_0) \tau''(n_0) = -1, \\ \tau'(0) = 0, \\ \tau(n^*) = 0, \end{cases} \quad (53)$$

and for $k > 1$,

$$\begin{cases} b(n_0) \tau'_k(n_0) + \frac{1}{2} \sigma^2(n_0) \tau''_k(n_0) = -k \tau_{k-1}(n_0), \\ \partial_{n_0} \tau_k(0) = 0, \\ \tau_k(n^*) = 0. \end{cases} \quad (54)$$

By direct integration, we can directly solve equation (53), which allows then to solve successively the sequence of problems (54). Write

$$\Psi(n_0) = e^{\int_0^{n_0} \frac{2b(n')}{\sigma^2(n')} dn'}. \quad (55)$$

Then, we have

$$\tau(n_0) = 2 \int_{n_0}^{n^*} \frac{1}{\Psi(y)} \int_0^y \frac{\Psi(z)}{\sigma^2(z)} dz dy. \quad (56)$$

In practice, denoting $\varepsilon > 0$ for the below bound instead of zero, we find

$$\Psi(n_0) = \left(\frac{n_0}{\varepsilon} \right)^{\frac{c}{a}} \exp \left(\frac{r}{a} n_0 - \frac{d}{\alpha \gamma a} e^{\alpha u} (1 - e^{-\alpha \gamma n_0}) \right).$$

Explicit computations lead to

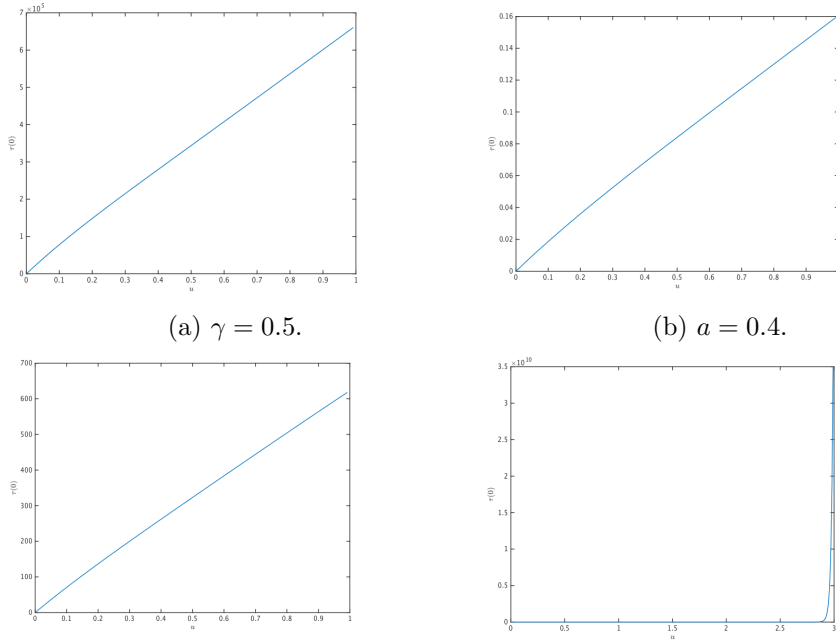


Figure 7: Mean first hitting times of a zero velocity as a function of u : depending on the parameters, the time is very large or reachable. Parameters: $\gamma = 0.5$, $\alpha = 0.8$, $c = 1$, $r = 0.6$, $d = 0.7$, $a = 0.1$. The figures below depict the same simulation on different scales.

$$\tau(n_0) = \frac{1}{a} \int_{n_0}^{n^*} \int_0^y \left(\frac{z}{y} \right)^{\frac{c}{a}} z^{-1} e^{\frac{r}{a}(z-y)} \exp \left(\frac{d}{a\alpha\gamma} e^{\alpha u} (e^{-\alpha\gamma z} - e^{-\alpha\gamma y}) \right) dz dy. \quad (57)$$

We perform numerical simulations of $\tau(0)$ for varying flow velocity u (see figure 7).

The simulations show that below a threshold flow velocity, the particle reaches a zero velocity very fast, while it gets extremely slow above the threshold. This dichotomy on u can be numerically modulated by γ corresponding to the adhesion force, and a corresponding to the noise. Increasing adhesion forces allows to stop cells in settings of higher flow, so as increasing the stochastic fluctuations due to the bonds dynamics.

7 Conclusions and perspectives

In this part, we have presented a discrete model for ligands binding on artery walls. The model is based on a stochastic description of the formation of weak bonds between the cell and the adhesive molecules on the wall, and of the stronger ones arising by self-reinforcement. This phenomenon

is modelled by a stochastic population model. The bonds dynamics are affected by the cell displacement by an interaction on their breaking rate: faster cells have shorter-lived bonds with the wall.

We are interested in the stopping time of the cell, that amounts to the first hitting time of a threshold value for the bond population. For this purpose, we derive a continuous model by scaling, so that the adhesion dynamics follows a diffusive stochastic differential equation. For constant parameters, no interaction or feedback is described, and the model resumes to a CIR process, for which properties of first hitting times are known. We provide its Laplace transform, and use a spectral method to make simulations of the corresponding probability density. Finally, for the model with interaction, we use a Fokker-Planck approach to have an integral formulation of the mean time to stop. Numerical simulations of this quantity as a function of the flow velocity show interesting results. First, a dichotomy appears in relation with the flow velocity: for low flows, the particle is stopped very fast, while above some threshold, the mean time to stop grows very steeply. Next, we checked that the simulations were the most sensitive on the adhesion coefficient γ , and on the stochastic parameter a . Indeed, larger adhesion forces favors the stopping of the cell. A larger noise also induces stops more easily, which is in agreement with the observations stated at the beginning.

Further works should emphasize on the comparison with experimental measures to enlighten conditions of stopping for the cell. Moreover, time-dependent rates will be considered to illustrate the effect of the heart cycle on the adhesion dynamics. Finally, this model can be extended to the case of adhesion to an adhesive surface in 2D. In this case, the position of adhesion proteins on the cell surface can not be neglected anymore. This situation will be handled by adding a spatial structure to the population of bonds, following the framework of [13, 8] and further works on measure-valued stochastic processes.

Acknowledgements the authors are very grateful to V.C. Tran, R. Voituriez for very helpful discussions and suggestions.

8 Appendice: Proof of proposition 3

Although the proof is similar to proposition 2.7 in [4] we recall it here for clarity. In the following C will denote a positive constant which value can change from line to line. The proof is split into three steps.

1. We know that $\mathbb{P} - a.s$, for a positive and measurable test function Φ ,

$$\begin{aligned}\Phi(N_t) &= \Phi(N_0) + \int_0^t \int_{\mathbb{R}_+} \left[(\Phi(N_{s^-} + 1) - \Phi(N_{s^-}) \mathbf{1}_{w \leq \lambda(N_{s^-})} \right. \\ &\quad \left. + (\Phi(N_{s^-} - 1) - \Phi(N_{s^-}) \mathbf{1}_{\lambda(N_{s^-}) \leq w \leq \lambda(N_{s^-}) + \mu(N_{s^-})}) \right] M(ds, dw),\end{aligned}$$

so that

$$\Phi(N_t) = \Phi(N_0) + \sum_{s \leq t} \Phi(N_{s^-} + (N_s - N_{s^-})) - \Phi(N_{s^-}). \quad (58)$$

Then, for $\Phi(N_t) = N_t^p$, using equation (4), and neglecting the negative death term, we get

$$N_t^p \leq N_0^p + \int_0^t \int_{\mathbb{R}_+} ((N_{s^-} + 1)^p - N_{s^-}^p) \mathbf{1}_{0 \leq u \leq \lambda(N_{s^-})} M(ds, dw).$$

For $n \geq 0$, consider the stopping time $\tau_n = \inf_{t \geq 0} \{N_t \geq n\}$. Then, taking expectations,

$$\begin{aligned}\mathbb{E} \left[\sup_{t \in [0, T \wedge \tau_n]} N_t^p \right] &\leq \mathbb{E}[N_0^p] + \mathbb{E} \left[\int_0^{T \wedge \tau_n} \lambda(N_{t^-}) ((N_{t^-} + 1)^p - N_{t^-}^p) dt \right], \\ &\leq \mathbb{E}[N_0^p] + \mathbb{E} \left[\int_0^{T \wedge \tau_n} C(1 + N_{t^-}) [(N_{t^-} + 1)^p - N_{t^-}^p] dt \right].\end{aligned}$$

We use now the following lemma, which can be proved by a direct computation:

Lemma 22. *Let $x \in \mathbb{R}_+$, and p a positive integer. Then, there exists a positive constant $C(p)$ such that*

$$(1 + x)^p - x^p \leq C(p)(1 + x^{p-1}).$$

Then,

$$\begin{aligned}\mathbb{E} \left[\sup_{t \in [0, T \wedge \tau_N]} N_t^p \right] &\leq \mathbb{E}[N_0^p] + C(p) \mathbb{E} \left[\int_0^{T \wedge \tau_N} (1 + N_{t^-}) (1 + N_{t^-}^{p-1}) dt \right] \\ &\leq \mathbb{E}[N_0^p] + C(p) \left(T + \int_0^T \mathbb{E} \left[\sup_{u \in [0, t \wedge \tau_N]} N_u^p \right] dt \right).\end{aligned}$$

We use now the Gronwall inequality together with the assumption on the initial term to get a partial result.

Let us now prove that $\lim_{n \rightarrow +\infty} \tau_n = +\infty$ $\mathbb{P} - a.s.$: if not, there exists $T^* < +\infty$ such that $\mathbb{P}(\sup_n \tau_n < T^*) > 0$. Then, by the Markov inequality, for all $n \in \mathbb{N}$, the following inequalities hold true:

$$\begin{aligned} \mathbb{E} \left[\sup_{t \in [0, T^* \wedge \tau_n]} N_t^p \right] &\geq \mathbb{P} \left(\sup_{t \in [0, T^* \wedge \tau_n]} N_t^p \geq n^p \right) n^p \\ &\geq \mathbb{P}(\tau_n < T^*) n^p \\ &\geq \underbrace{\mathbb{P} \left(\sup_n \tau_n < T^* \right)}_{>0} n^p, \end{aligned}$$

which contradicts the previous inequality since $\mathbb{E} \left[\sup_{t \in [0, T \wedge \tau_n]} N_t^p \right]$ was bounded independantly of n . Finally, by the Fatou inequality:

$$\begin{aligned} \mathbb{E} \left[\sup_{t \in [0, T]} N_t^p \right] &= \mathbb{E} \left[\liminf_{n \rightarrow +\infty} \sup_{t \in [0, T \wedge \tau_n]} N_t^p \right] \\ &\leq \liminf_{n \rightarrow +\infty} \mathbb{E} \left[\sup_{t \in [0, T \wedge \tau_n]} N_t^p \right] \leq C(p, T) < +\infty. \end{aligned}$$

2. Let $T_0 = 0$ be the first time of event, and $t \in \mathbb{R}_+$. Then, the global jump rate of N_t is smaller than $\bar{C} + (\bar{R} + \bar{D})N_t \leq C(1 + N_t)$. One can $\mathbb{P} - a.s.$ define the sequence $(T_k)_{k \in \mathbb{N}^*}$ of jumping times, as well as $T_\infty := \lim_{k \rightarrow +\infty} T_k$. By definition, the process $(N_t)_t$ can be inductively constructed on $[0, T_\infty[$. Showing existence of a solution $(N_t)_{t \in \mathbb{R}_+} \in \mathbb{D}(\mathbb{R}_+, \mathbb{R}_+)$ amounts to showing that $\mathbb{P} - a.s.$, $T_\infty = +\infty$. From the first step, the population size stays controlled in finite time. As a consequence, the appearance of events can be compared to a Poisson variable, leading to the result.
3. Uniqueness is clear by construction. It is possible to derive a rigorous proof by induction, using the trajectorial representation of the process. We do not detail this here.

9 Appendice: Proof of proposition 4

1. This is a direct consequence of Dynkin's theorem combined with the integrability of each term, and the assumption on the initial condition.
2. Take $N \in \mathbb{R}_+$ and $\Phi(N) = N^q$ for $0 \leq q \leq p$. Then,

$$|\Phi(N)| + |L\Phi(N)| \leq N^q + (\bar{C} + \bar{R}N) |(N+1)^q - N^q| + \bar{D}N |(N-1)^q - N^q|.$$

Now notice that as $|(N + 1)^q - N^q| \leq C(1 + N^{q-1})$ and $|(N - 1)^q - N^q| \leq C(1 + N^{q-1})$,

$$|\Phi(N)| + |L\Phi(N)| \leq C(1 + N^q).$$

3. Let us now prove the semimartingale formulation. We first notice that expression (7) comes from (6) for $\Phi_1(N) := N$. Now, let us compute the quadratic variation of this martingale.

→ As a first step, compute the Doob decomposition of $\Phi(N_t) := N_t^2$ using equation (6). We can write

$$L\Phi(N) = [\lambda(N) + \mu(N)] + 2N [\lambda(N) - \mu(N)].$$

By point 2, we have that

$$N_t^2 - N_0^2 - \int_0^t \lambda(N_s) + \mu(N_s) + 2N_s [\lambda(N_s) - \mu(N_s)] ds$$

is a càdlàg martingale starting from 0.

→ Now, applying Itô's formula to equation (7) leads to another decomposition that involves the quadratic variation of $(M_t)_t$:

$$N_t^2 - N_0^2 - \int_0^t 2N_s [\lambda(N_s) - \mu(N_s)] ds - \langle M \rangle_t$$

is a martingale. From uniqueness of such a decomposition, we find that

$$\langle M \rangle_t = \int_0^t \lambda(N_s) + \mu(N_s) ds,$$

that is exactly equation (8).

References

- [1] JOSEPH ABATE AND WARD WHITT, *The Fourier-series method for inverting transforms of probability distributions*, Queueing systems, 10, 5–87, (1992).
- [2] DAVID ALDOUS, *Stopping Times and Tightness. II*, The Annals of Probability, 17, 586-595, (1989).
- [3] KRISHNA ATHREYA AND PETER NEY, *Branching processes*, Die Grundlehren der mathematischen Wissenschaften, 196, (1972).
- [4] VINCENT BANSAYE AND SYLVIE MÉLÉARD, *Some stochastic models for structured populations : scaling limits and long time behavior*, (2015).

- [5] G. BELL, *Models for the specific adhesion of cells to cell*, Science, 200:618627, 1978.
- [6] ABDEL BERKAOUI, MIREILLE BOSSY AND AWA DIOP, *Euler scheme for SDEs with non-Lipschitz diffusion coefficient: strong convergence*, ESAIM: PS, 12, 1-11, (2008).
- [7] SUJATA K BHATIA, MICHAEL R KING AND DANIEL A HAMMER, *The state diagram for cell adhesion mediated by two receptors*, Biophysical journal, 84, 2671–2690, (2003).
- [8] NICOLAS CHAMPAGNAT AND SYLVIE MÉLÉARD, *Invasion and adaptive evolution for individual-based spatially structured populations*, Journal of Mathematical Biology, 55, 147–188, (2007).
- [9] KAI-CHIEN CHANG AND DANIEL HAMMER, *The forward rate of binding of surface-tethered reactants: effect of relative motion between two surfaces*, Biophysical Journal, 76, 1280–1292, (1999).
- [10] DMITRY DAVYDOV AND VADIM LINETSKY, *Pricing options on scalar diffusions: an eigenfunction expansion approach*, Operations research, 51, 185–209, (2003).
- [11] STEWART ETHIER AND THOMAS KURTZ, *Markov processes: characterization and convergence*, John Wiley & Sons, 282, (2009).
- [12] ANJA GÖING-JAESCHKE AND MARC YOR, *A Survey and Some Generalizations of Bessel Processes*, Bernoulli, 9, 313–349, (1999).
- [13] NICOLAS FOURNIER AND SYLVIE MÉLÉARD, *A microscopic probabilistic description of a locally regulated population and macroscopic approximations*, The Annals of Applied Probability, 14, (2004).
- [14] DOUGLAS GOETZ, MARWAN EL-SABBAN, BENDICHT PAULI AND DANIEL HAMMER, *Dynamics of neutrophil rolling over stimulated endothelium in vitro.*, Biophysical journal, 66, (1994).
- [15] NEIL GRANGER AND ELENA SENCHENKOVA, *Inflammation and the Microcirculation*, Colloquium Series on Integrated Systems Physiology: From Molecule to Function, 2, 1–87, (2010).
- [16] BÉRÉNICE GREC, BERTRAND MAURY, NICOLAS MEUNIER AND LAURENT NAVORET, *The role of ligands binding in shear induced leukocyte rolling* (2012).
- [17] DANIEL HAMMER AND S. APTE, *Simulation of cell rolling and adhesion on surfaces in shear flow: general results and analysis of selectin-mediated neutrophil adhesion*, Biophys. J., 63(1):3357, 1992.

- [18] D. HAMMER AND D. LAUFFENBURGER, *A dynamical model for receptor-mediated cell adhesion to surfaces*, *Biophys. J.*, 52:475487, 1987.
- [19] N IKEDA AND S WATANABE, *Stochastic differential equations and diffusion processes*, Kodansha scientific books, North-Holland, (1989).
- [20] K ITÔ AND HENRY P MCKEAN, *Diffusion Processes and Their Sample Paths*, *Grundlehren der Mathematischen Wissenschaften*, 125, (1965).
- [21] SAMEER JADHAV, CHARLES D EGGLETON, AND KONSTANTINOS KONSTANTOPOULOS, *A 3-D computational model predicts that cell deformation affects selectin-mediated leukocyte rolling*, *Biophysical journal*, 88, 96–104, (2005).
- [22] A JOFFE AND M METIVIER, *Weak Convergence of Sequences of Semimartingales with Applications to Multitype Branching Processes*, *Advances in Applied Probability*, 18, (1986).
- [23] IOANNIS KARATZAS AND STEVEN E SHREVE, *Brownian Motion and Stochastic Calculus*, *Graduate Texts in Mathematics*, Springer New York, New York, NY, (1998)
- [24] C. KORN, *Stochastic dynamics of cell adhesion in hydrodynamic flow*, PhD thesis, Universitat Potsdam, 2007.
- [25] C. B. KORN AND U. S. SCHWARZ, *Dynamic states of cells adhering in shear flow: From slipping to rolling*, *Phys. Rev. E*, 77:041904, 2008.
- [26] BORIS LEBLANC AND OLIVIER SCAILLET, *Path dependent options on yields in the affine term structure model*, *Finance and Stochastics*, 2, 349–367, (1998).
- [27] KLAUS LEY, CARLO LAUDANNA, MYRON I CYBULSKY AND SUSSAN NOURSHARGH, *Getting to the site of inflammation: the leukocyte adhesion cascade updated*, *Nature Reviews Immunology*, 7, 678–689, (2007).
- [28] VADIM LINETSKY, *Computing hitting time densities for CIR and OU diffusions: Applications to mean-reverting models*, *Journal of Computational Finance*, 7, 1–22, (2004).
- [29] VADIM LINETSKY, *Lookback options and diffusion hitting times: A spectral expansion approach*, *Finance and Stochastics*, 8, 373–398, (2004).
- [30] VADIM LINETSKY, *The spectral decomposition of the option value*, *International Journal of Theoretical and Applied Finance*, 7, 337–384, (2004).
- [31] HENRY MCKEAN, *Elementary solutions for certain parabolic partial differential equations*, (1956).

- [32] VUK MILIŠIĆ AND DIETMAR OELZ, *On the asymptotic regime of a model for friction mediated by transient elastic linkages*, Journal de mathématiques pures et appliquées, 96, 484–501 (2011).
- [33] VUK MILIŠIĆ AND DIETMAR OELZ, *On a structured model for load-dependent reaction kinetics of transient elastic linkages mediating non-linear friction*, SIAM Journal on Mathematical Analysis, 47, 2104–2121 (2015).
- [34] ALICE NICOLAS, BENJAMIN GEIGER AND SAMUEL A SAFRAN, *Cell mechanosensitivity controls the anisotropy of focal adhesions*, Proceedings of the National Academy of Sciences of the United States of America, 101, 12520–12525, (2004).
- [35] JIM PITMAN AND MARC YOR, *Bessel processes and infinitely divisible laws*, Stochastic integrals, 285–370, Springer, (1981)
- [36] L. PREZIOSI AND G. VITALE, *Mechanical aspects of tumour growth: Multiphase modelling, adhesion, and evolving natural configurations*, in M. Ben Amar, A. Goriely, M. M. Müller, L. F. Cugliandolo, Eds., New Trends in the Physics and Mechanics of Biological Systems, p. 177-228, Lecture Notes of the Les Houches Summer School, vol. 92, Oxford University Press., 2011.
- [37] DANIEL REVUZ AND MARC YOR, *Continuous martingales and Brownian motion*, 293, Springer, Berlin (2005)
- [38] GEERT SCHMID-SCHÖÖUNBEIN, RICHARD SKALAK, SCOTT SIMON AND ROBERT ENGLER, *The Interaction between Leukocytes and Endothelium in Vivo*, Annals of the New York Academy of Sciences, 516, 348–361, (1987).
- [39] ANQI SHAO, *A fast and exact simulation for CIR process*, University of Florida, (2012)
- [40] STEVEN SHREVE, *Stochastic calculus for finance II: Continuous-time models*, Springer Science & Business Media, (2004)
- [41] TIMOTHY SPRINGER AND OTHERS, *Adhesion receptors of the immune system*, Nature, 346, 425–434, (1990).
- [42] VIET CHI TRAN, *Modèles particuliers stochastiques pour des problèmes d'évolution adaptative et pour l'approximation de solutions statistiques*, phdthesis, Université Paris X, (2006)
- [43] DIETMAR VESTWEBER, *How leukocytes cross the vascular endothelium*, Nature Reviews Immunology (2015).

- [44] YIHUA ZHAO, SHO CHIEN, AND RICHARD SKALAK, *A stochastic model of leukocyte rolling*, Biophysical journal, 69 (1995).